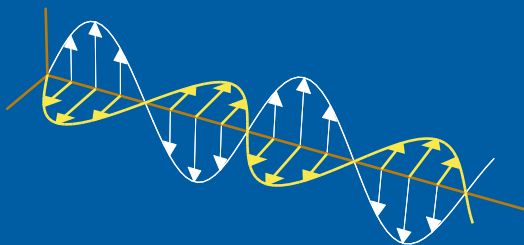# State-space models and stored electromagnetic energy for antennas in dispersive and heterogeneous media

Mats Gustafsson and Casimir Ehrenborg

Electromagnetic Theory
Department of Electrical and Information Technology
Lund University
Sweden

Mats Gustafsson
mats.gustafsson@eit.lth.se

Department of Electrical and Information Technology
Electromagnetic Theory
Lund University
P.O. Box 118
SE-221 00 Lund
Sweden

Casimir Ehrenborg
casimir.ehrenborg@eit.lth.se

Department of Electrical and Information Technology
Electromagnetic Theory
Lund University
P.O. Box 118
SE-221 00 Lund
Sweden

Abstract

Accurate and efficient evaluation of the stored energy is essential for Q-factors, physical bounds, and antenna current optimization. Here, it is shown that the stored energy can be estimated from quadratic forms based on a state-space representation derived from the electric and magnetic field integral equations. The derived expressions are valid for small antennas embedded in temporally dispersive and inhomogeneous media. The quadratic forms also provide simple single frequency formulas for the corresponding Q-factors. Numerical examples comparing the different Q-factors are presented for dipole and meander line antennas in conductive, Debye, and Lorentz media for homogeneous and inhomogeneous media. The computed Q-factors are also verified with the Q-factor obtained from the stored energy in Brune synthesized circuit models.

1 Introduction

Antennas are placed in the proximity of, or inside, lossy media in applications involving mobile phones, body area networks, implants, submarines, and plasmonics [2, 41, 54]. The losses in such systems are associated with conduction or relaxation phenomena. These effects lead to a frequency dependent permittivity, and hence temporal dispersion. Temporal dispersion is present in natural [4, 33, 39] and artificial materials [6, 9, 15]. Dispersion can often be neglected for antenna modeling in the microwave range, but it is usually necessary for modeling of phenomena in the mm, THz, and optical range. Electromagnetic energy density in dispersive media builds on the classical results in [39] with extensions to applications such as antennas, metamaterials, and photonics [45, 48, 53, 58].

Stored energy is instrumental for antenna analysis in terms of the Q-factor [8, 11, 14, 24, 27, 51, 59]. In [29, 57, 58] stored energy is considered for small antennas composed of dispersive or lossy media, embedded in free space. However, when calculating stored energy for antennas embedded in lossy background media, new challenges arise. The classical subtraction technique, where the energy in the far-field is subtracted from the total energy density, is difficult to generalize to lossy media due to the exponential decay of the far-field and its associated coordinate dependence [42]. Here, we follow the approach [17, 31, 49] and express the stored energy and Q-factors in terms of the current density on the antenna structure. The derivation is based on a state-space representation [55] together with frequency differentiation of the method of moments (MoM) impedance matrix.

Stored energy is investigated for state-space models in [55], where it is shown that the stored energy is associated with minimal systems having internal symmetry, *i.e.*, reciprocity. We use this approach to construct symmetric state-space models for antennas in dispersive media, and calculate their stored energy. The explicit results are given for conductivity, Debye, Drude, and Lorentz models and are simply generalized to models with multiple terms [4, 33, 39]. The resulting models are classical state-space models for small antennas, but contain a phase shift (time delay) for larger structures that is not considered in [55]. Here, we use a local approximation based on differentiation with respect to the frequency to include time-delay effects [26]. In total, this offers a stored energy that is identical to the stored energy defined by subtraction of the far-field energy term for the free space coordinate independent case [22]. Moreover, the stored energy derived from the state-space model in dispersive media equals the stored energy determined from synthesized circuit models for small antennas.

This paper is organized as follows. In Sec. 2, the Q-factor and stored energies are discussed. A state-space model based on the MoM impedance matrix and its stored energy is introduced in Sec. 3. The state-space models and stored energies are generalized to temporally dispersive and inhomogeneous media in Secs 4 and 5, respectively. The paper is concluded in Sec. 6. The symbol (🜚) is used to indicate that a figure can be animated.
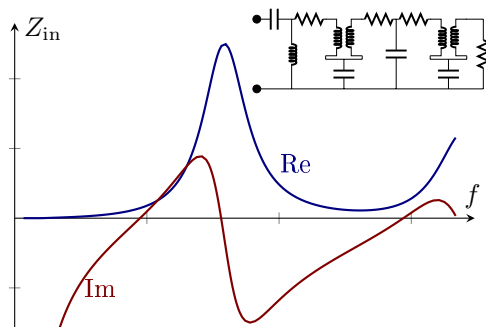
Figure 1: The three different approaches to express stored energy, electromagnetic fields, current density, and input impedance. Here all are illustrated for the same capacitive dipole. a) snapshot of the magnetic field around the antenna. b) stored energy density around the antenna. c) current density on the antenna. d) input impedance and circuit model for the antenna.

2 Stored energy, Q factor, and state-space models

Stored energy for antennas is a concept which arose by necessity to calculate the Q-factor [11, 27, 43, 51, 59]. The Q-factor measures how well an oscillating system stores energy as opposed to dissipating it. The Q-factor for an antenna tuned to resonance is defined as [27, 51, 59]

$$Q = \frac{2\omega \max\{W_{\mathrm{e}}, W_{\mathrm{m}}\}}{P_{\mathrm{d}}} = \omega \frac{W + |W_{\mathrm{m}} - W_{\mathrm{e}}|}{P_{\mathrm{d}}}, \tag{2.1}$$

where $W = W_{\mathrm{e}} + W_{\mathrm{m}}$, W_{e}, and W_{m} denote the stored electromagnetic, electric, and magnetic energies, respectively, ω is the angular frequency, and P_{d} is the dissipated power. The dissipated power P_{d} and energy difference $W_{\mathrm{m}} - W_{\mathrm{e}}$ are well defined and follows directly from Poynting's theorem [19, 22]. Because of its relation to the bandwidth the Q-factor is an important parameter for antenna design. Thus it has become imperative to define stored energy for antennas [8, 11, 27, 51, 59]. However, this is not trivial as electromagnetic fields, current densities, and circuit models can give different interpretations of the stored energy, see Fig. 1. In this section follows a brief overview of previous methods used to define stored energy.

The classical way of interpreting stored energy is as the energy stored in the fields that radiate from the antenna, but do not escape its vicinity, see Fig. 1b. This naturally leads to the subtraction calculation method, where the stored energy, W_{F}, is calculated by subtracting the power flow or the far-field power from the total energy [14, 16, 27, 51, 59]. Subtraction of the far-field term yields

$$W_{\mathrm{F}} = \frac{1}{4} \int_{\mathbb{R}^3_{\mathrm{r}}} \epsilon |\boldsymbol{E}(\boldsymbol{r})|^2 + \mu |\boldsymbol{H}(\boldsymbol{r})|^2 - 2\epsilon \frac{|\boldsymbol{F}(\hat{\boldsymbol{r}})|^2}{r^2} \, \mathrm{dV}, \tag{2.2}$$

where ϵ is the permittivity, μ is the permeability, $\boldsymbol{E}$ and $\boldsymbol{H}$ are the electric and magnetic fields,

and $\boldsymbol{F}(\hat{\boldsymbol{r}})$ is the electric far-field; $\boldsymbol{F} \sim \mathrm{e}^{\mathrm{j}kr}r\boldsymbol{E}$ as $r \to \infty$ with $r = |\boldsymbol{r}|$ and $\hat{\boldsymbol{r}} = \boldsymbol{r}/r$. This definition of stored energy has been generally accepted since the classical work by Collin and Rothschild [14], see also [16, 40, 59]. The stored energy (2.2) can also be expressed in the current density on the antenna structure [18, 22, 49, 50], see Fig. 1c. This simplifies the evaluation of stored energy and enables antenna current optimization [7, 23, 24, 25, 34]. The main drawbacks with (2.2) are possible coordinate dependence [22, 59] and negative stored energies [25, 59]. Moreover, as soon as losses are introduced in the background material, the far-field vanishes, *i.e.*, $\boldsymbol{F}(\hat{\boldsymbol{r}}) = \boldsymbol{0}$. This implies that W_{F} equals the total energy and it is hence not possible to distinguish the stored energy from the total energy in lossy backgrounds using (2.2) [59].

Using the same concept of stored energy defined as energy in the fields around the antenna, subtraction of the power flow from the energy density suggests the stored energy

$$W_{\mathrm{P}} = \frac{1}{4} \int_{\mathbb{R}_{\mathrm{r}}^3} \epsilon|\boldsymbol{E}(\boldsymbol{r})|^2 + \mu|\boldsymbol{H}(\boldsymbol{r})|^2 - 4|\sqrt{\epsilon\mu}\boldsymbol{P}(\boldsymbol{r})|\,\mathrm{dV}, \tag{2.3}$$

where $\boldsymbol{P} = \frac{1}{2}\mathrm{Re}\{\boldsymbol{E} \times \boldsymbol{H}^*\}$ is the time-average Poynting vector. This definition is coordinate independent and can be used in inhomogeneous and lossy backgrounds. However, the integral needs to be evaluated numerically and it is not clear how to generalize the formulation to temporally dispersive backgrounds. As an alternative, the radial component of the Poynting vector $\hat{\boldsymbol{r}} \cdot \boldsymbol{P}$ can be subtracted instead of the far-field amplitude [14, 40]. This leads to a coordinate dependent expression that differs from (2.2) by the radiated energy of the standing waves within the structure [22].

The problems with (2.2) and (2.3) call for alternative methodologies to define and evaluate the stored energy. To circumvent some of these problems, we consider the stored energy for the antenna as the stored energy seen from the input impedance, Z_{in}, see Fig. 1d. This has several advantages, such as being related to the impedance bandwidth, coordinate independent, and valid in arbitrary surrounding materials.

The input-impedance is separated into a resistive and reactive part, where the resistive part relates to dissipated energy and the reactive part relates to stored energy. For a lumped circuit network the reactance is proportional to the difference between energy stored capacitively and energy stored inductively

$$Z_{\mathrm{in}} = R_{\mathrm{in}} + \mathrm{j}X_{\mathrm{in}} = \frac{2P_{\mathrm{d}} + 4\mathrm{j}\omega(W_{\mathrm{m}} - W_{\mathrm{e}})}{|I_{\mathrm{in}}|^2}, \tag{2.4}$$

where R_{in} is the input resistance, X_{in} the input reactance, and I_{in} the input current. The input impedance of the antenna can be modeled with circuit elements using, *e.g.*, Brune synthesis [5, 21], see also Fig. 1d. Kirchoff's laws are used to relate the currents $\mathbf{I}$ and voltages $\mathbf{V} = \mathbf{Z}\mathbf{I}$ via the impedance matrix $\mathbf{Z}$, in the circuit network. The impedance matrix is further decomposed in its resistance $\mathbf{R}$, inductance $\mathbf{L}$, and capacitance $\mathbf{C} = \mathbf{C}_{\mathrm{i}}^{-1}$ matrices:

$$\mathbf{Z} = \mathbf{R} + \mathrm{j}\mathbf{X} = \mathbf{R} + \mathrm{j}\omega\mathbf{L} + \frac{1}{\mathrm{j}\omega}\mathbf{C}_{\mathrm{i}} = \mathbf{R} + s\mathbf{L} + \frac{1}{s}\mathbf{C}_{\mathrm{i}}, \tag{2.5}$$

where s is the Laplace parameter. The impedance matrix (2.5) can be considered as a second order state-space model for the input impedance $Z_{\mathrm{in}} = V_{\mathrm{in}}/I_{\mathrm{in}}$ with the input $\mathbf{V} = \mathbf{B}V_{\mathrm{in}}$ and output $I_{\mathrm{in}} = \mathbf{B}^{\mathrm{T}}\mathbf{I}$, where the superscript $^{\mathrm{T}}$ denotes the transpose. For the analysis in the paper, the second order state-space model (2.5) is rewritten as the first order model [55]

$$s\begin{pmatrix} \mathbf{L} & \mathbf{0} \\ \mathbf{0} & \mathbf{C} \end{pmatrix}\begin{pmatrix} \mathbf{I} \\ \mathbf{U} \end{pmatrix} + \begin{pmatrix} \mathbf{R} & \mathbf{1} \\ -\mathbf{1} & \mathbf{0} \end{pmatrix}\begin{pmatrix} \mathbf{I} \\ \mathbf{U} \end{pmatrix} = \begin{pmatrix} s\mathbf{L}+\mathbf{R} & \mathbf{1} \\ -\mathbf{1} & s\mathbf{C} \end{pmatrix}\begin{pmatrix} \mathbf{I} \\ \mathbf{U} \end{pmatrix} = \begin{pmatrix} \mathbf{V} \\ \mathbf{0} \end{pmatrix} \quad \text{or} \quad \widetilde{\mathbf{Z}}\widetilde{\mathbf{I}} = \widetilde{\mathbf{V}}, \tag{2.6}$$

where the voltage state $\mathbf{U} = \frac{1}{s}\mathbf{C}_{\mathrm{i}}\mathbf{I}$ is introduced, and $\mathbf{1}$ is the identity matrix. The time-domain $(s \to \frac{\partial}{\partial t})$ stored energy is defined from the energy balance that is derived by multiplication of (2.6) with the states, $(\mathbf{I}\ \mathbf{U})^{\mathrm{T}}$, from the left and temporal integration, *i.e.*,

$$\left[\frac{\mathbf{I}^{\mathrm{T}}(t)\mathbf{L}\mathbf{I}(t) + \mathbf{U}^{\mathrm{T}}(t)\mathbf{C}\mathbf{U}(t)}{2}\right]_{t_1}^{t_2} + \int_{t_1}^{t_2} \mathbf{I}^{\mathrm{T}}(t)\mathbf{R}\mathbf{I}(t)\,\mathrm{dt} = \int_{t_1}^{t_2} \mathbf{I}^{\mathrm{T}}(t)\mathbf{V}(t)\,\mathrm{dt}, \tag{2.7}$$

where for notational simplicity the time t is used to define time-domain quantities. The first and second terms in the left-hand side are identified as the change of stored energy and dissipated energy during the time interval $[t_1, t_2]$, respectively. The right-hand side is the supplied energy during the same period. The time-average stored energy for a time-harmonic signal in (2.7) is alternatively obtained from the quadratic form constructed from the matrix multiplying s in (2.6), *i.e.*,

$$W = \frac{\mathbf{I}^{\mathrm{H}}\mathbf{LI}}{4} + \frac{\mathbf{U}^{\mathrm{H}}\mathbf{CU}}{4} = \frac{\mathbf{I}^{\mathrm{H}}\mathbf{LI}}{4} + \frac{\mathbf{I}^{\mathrm{H}}\mathbf{C}_{\mathrm{i}}^{\mathrm{H}}\mathbf{CC}_{\mathrm{i}}\mathbf{I}}{4\omega^2} = \frac{1}{4}\mathbf{I}^{\mathrm{H}}\left(\mathbf{L} + \frac{\mathbf{C}_{\mathrm{i}}}{\omega^2}\right)\mathbf{I} = \frac{\mathbf{I}^{\mathrm{H}}\mathbf{X}'\mathbf{I}}{4} = \frac{\tilde{\mathbf{I}}^{\mathrm{H}}\widetilde{\mathbf{X}}'\tilde{\mathbf{I}}}{4}, \quad (2.8)$$

where the superscripts $^{\mathrm{H}}$ and prime $'$ denotes the conjugate transpose and differentiation with respect to ω, respectively, and $\widetilde{\mathbf{Z}} = \widetilde{\mathbf{R}} + \mathrm{j}\widetilde{\mathbf{X}}$. It is essential that the matrices $\mathbf{L} = \mathbf{L}^{\mathrm{T}}$ and $\mathbf{C}_{\mathrm{i}} = \mathbf{C}_{\mathrm{i}}^{\mathrm{T}}$ are symmetric, frequency independent, and real valued to determine the stored energy [55].

The stored energy expression (2.8) is a Hermitian quadratic form in terms of the frequency derivative of the reactance or state-space reactance matrix. The difference between the stored magnetic and electric energies (2.4) gives the explicit formulas for the stored magnetic and electric energies

$$W_{\mathrm{m}} = \frac{1}{8}\mathbf{I}^{\mathrm{H}}\left(\frac{\partial \mathbf{X}}{\partial \omega} + \frac{\mathbf{X}}{\omega}\right)\mathbf{I} = \frac{1}{4}\mathbf{I}^{\mathrm{H}}\mathbf{LI} \quad (2.9)$$

and

$$W_{\mathrm{e}} = \frac{1}{8}\mathbf{I}^{\mathrm{H}}\left(\frac{\partial \mathbf{X}}{\partial \omega} - \frac{\mathbf{X}}{\omega}\right)\mathbf{I} = \frac{1}{4\omega^2}\mathbf{I}^{\mathrm{H}}\mathbf{C}_{\mathrm{i}}\mathbf{I}, \quad (2.10)$$

respectively. The stored energy (2.8) can hence be interpreted as the sum of the electric energy in the capacitors and the magnetic energy in the inductors. The relations (2.9) and (2.10) resemble the expressions in [19, 30] for the input impedance of single and array antennas. Here, it is essential to note that (2.9) and (2.10) are expressed in the state-space matrix and not in the input impedance, *cf.*, [19, 30]. The expressions based on the input impedance are only valid for single resonance RLC circuits and lossless circuit networks [30]. The Brune synthesized circuit and the state-space representation are mathematical models created from a rational approximation of the input impedance. Here, it is also important to realize that the circuit model is non-unique and that there are several methods to synthesize circuit models [56].

The Q-factor (2.1) is expressed in the reactance matrix and its frequency derivative as

$$Q = \frac{\max\{\mathbf{I}^{\mathrm{H}}(\omega\mathbf{X}' \pm \mathbf{X})\mathbf{I}\}}{2\mathbf{I}^{\mathrm{H}}\mathbf{RI}} = \frac{\omega\mathbf{I}^{\mathrm{H}}\mathbf{X}'\mathbf{I} + |\mathbf{I}^{\mathrm{H}}\mathbf{XI}|}{2\mathbf{I}^{\mathrm{H}}\mathbf{RI}}, \quad (2.11)$$

where we used the time average dissipated power $P_{\mathrm{d}} = \frac{1}{2}\operatorname{Re}\{\mathbf{I}^{\mathrm{H}}\mathbf{V}\} = \frac{1}{2}\mathbf{I}^{\mathrm{H}}\mathbf{RI}$. The Q-factor (2.11) is determined from the input impedance (2.4) and hence related to the fractional bandwidth of the antenna. However, the dependence on the input impedance is also the main draw back of this method, as it is based on the antenna geometry including its feed. In this paper we view the antenna as a black box system, but instead of synthesizing an equivalent circuit model we create a state-space model based on the MoM impedance matrix.

We consider antennas in an inhomogeneous temporally dispersive background medium, see Fig. 2. The background medium has permittivity $\epsilon = \epsilon_0\epsilon_{\mathrm{r}}$ and permeability $\mu = \mu_0\mu_{\mathrm{r}}$ which depend on the angular frequency ω or Laplace parameter $s = \mathrm{j}\omega$. The wave impedance $\eta = \sqrt{\mu/\epsilon}$, the index of refraction $n = \sqrt{s^2\epsilon_{\mathrm{r}}\mu_{\mathrm{r}}}/s$, the wavenumber $k = -\mathrm{j}\kappa$, where $\kappa = \sqrt{s^2\epsilon\mu}$, speed of light $\mathrm{c}_0 = 1/\sqrt{\epsilon_0\mu_0}$, and the intrinsic impedance of vacuum $\eta_0 = \sqrt{\mu_0/\epsilon_0}$ are also used to simplify the notation. To start, we restrict the analysis to electric surface current densities in free space in Sec. 3. This case is thoroughly analyzed using (2.2) in [21, 22, 49, 50]. The background material is subsequently generalized to temporally dispersive in Sec. 4, piecewise inhomogeneous in Sec. 5.1, and inhomogeneous in Sec. 5.2.
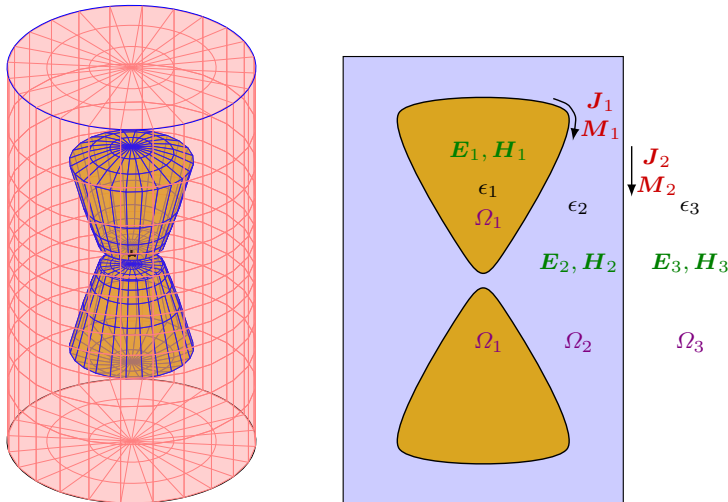
Figure 2: Illustration of an antenna geometry composed of three materials modeled by their permittivity ϵ_n and permeability μ_n, $n = 1, 2, 3$ in the regions Ω_n. The electromagnetic fields are denoted $\boldsymbol{E}_n$ and $\boldsymbol{H}_n$ in Ω_n. The equivalent (surface) currents $\boldsymbol{J}_m$ and $\boldsymbol{M}_m$ have support on the boundary between Ω_m and Ω_{m+1}, $m = 1, 2$. (left) three dimensional and (right) two dimensional cut.

3 Stored energy for antennas in free space

The state-space model is based on the electric field integral equation (EFIE) impedance matrix $\mathbf{Z}$. A standard MoM implementation of the EFIE determines the impedance matrix [10, 44, 52] which can be written as

$$\mathbf{Z} = s\mu\mathbf{L} + \frac{1}{s\epsilon}\mathbf{C}_i = \eta\kappa\mathbf{L} + \frac{\eta}{\kappa}\mathbf{C}_i, \tag{3.1}$$

where the matrices $\mathbf{L}$ and $\mathbf{C}_i$ depend on the wavenumber and have the elements

$$L_{mn} = \int_{\partial\Omega}\int_{\partial\Omega} \boldsymbol{\psi}_m(\boldsymbol{r}_1) \cdot \boldsymbol{\psi}_n(\boldsymbol{r}_2) \frac{\mathrm{e}^{-\mathrm{j}kR_{12}}}{4\pi R_{12}} \, \mathrm{dS}_1 \, \mathrm{dS}_2 \tag{3.2}$$

and

$$C_{imn} = \int_{\partial\Omega}\int_{\partial\Omega} \nabla_1 \cdot \boldsymbol{\psi}_m(\boldsymbol{r}_1)\nabla_2 \cdot \boldsymbol{\psi}_n(\boldsymbol{r}_2) \frac{\mathrm{e}^{-\mathrm{j}kR_{12}}}{4\pi R_{12}} \, \mathrm{dS}_1 \, \mathrm{dS}_2, \tag{3.3}$$

where $R_{12} = |\boldsymbol{r}_1 - \boldsymbol{r}_2|$ is the distance between the spatial points $\boldsymbol{r}_1$ and $\boldsymbol{r}_2$ and $\partial\Omega$ denotes the antenna boundary modeled as a perfect electric conductor (PEC). The material parameters are $\epsilon = \epsilon_0$ and $\mu = \mu_0$ for the free space case. The basis functions, $\boldsymbol{\psi}_m(\boldsymbol{r})$, are assumed to be real valued and divergence conforming with vanishing normal components at the antenna boundary [30, 44]. The decomposition of the MoM impedance matrix (3.1) resembles the impedance matrix for lumped circuits (2.5) with the major differences that $\mathbf{R}$ is missing and that $\mathbf{L}$ and $\mathbf{C}_i$ are complex valued and depend on s in (3.1). The MoM impedance matrix (3.1) can alternatively be decomposed as (2.5) using the real and imaginary parts, see App. B. It is however advantageous to keep (3.1) for the presentation in this paper.

The state-space model is constructed for the input impedance, $Z_{\mathrm{in}} = V_{\mathrm{in}}/I_{\mathrm{in}}$, with the voltage excitation V_{in} and current output I_{in}. The current column matrix $\mathbf{I}$ contains the expansion coefficients I_n for the current density $\boldsymbol{J}(\boldsymbol{r}) = \sum_{n=1}^{N} I_n \boldsymbol{\psi}_n(\boldsymbol{r})$ that is determined from the linear system

$$\mathbf{ZI} = \mathbf{V} = \mathbf{B}V_{\mathrm{in}} \quad \text{and} \quad I_{\mathrm{in}} = \mathbf{B}^{\mathrm{T}}\mathbf{I}. \tag{3.4}$$

Inspired by the stored energy in circuit models (2.8) and more general state-space models [55], we use a state-space approach to determine the stored energy for antennas. This changes the

interpretation of stored energy from energy stored in the electromagnetic fields to energy stored in the sources (states), see Fig.1. The state-space model also shows that the stored energy determined from the current density is related to the stored energy determined from the input impedance for small antennas $ka \ll 1$, where a denotes the radius of the smallest circumscribing sphere [11].

A PEC antenna structure embedded in a homogeneous isotropic media is modeled by the EFIE (3.1) and (3.4). The system can be written

$$\mathbf{ZI} = (s\mu\mathbf{L} + \frac{1}{s\epsilon}\mathbf{C}_i)\mathbf{I} = s\mu\mathbf{LI} + \mathbf{U} = \mathbf{V} = \mathbf{B}V_{in} \quad \text{and} \quad I_{in} = \mathbf{B}^T\mathbf{I}, \tag{3.5}$$

where a voltage state $\mathbf{U} = \frac{1}{s\epsilon}\mathbf{C}_i\mathbf{I}$ is introduced, $cf.$, (2.6), to rewrite the second order system (3.5) to the first order system

$$s\begin{pmatrix} \mu\mathbf{L} & \mathbf{0} \\ \mathbf{0} & \epsilon\mathbf{C} \end{pmatrix}\begin{pmatrix} \mathbf{I} \\ \mathbf{U} \end{pmatrix} = \begin{pmatrix} \mathbf{0} & -\mathbf{1} \\ \mathbf{1} & \mathbf{0} \end{pmatrix}\begin{pmatrix} \mathbf{I} \\ \mathbf{U} \end{pmatrix} + \begin{pmatrix} \mathbf{B} \\ \mathbf{0} \end{pmatrix}V_{in}. \tag{3.6}$$

The system is a classical state-space model for the free space case, $\epsilon = \epsilon_0$ and $\mu = \mu_0$, in the limit of small antennas $ka \ll 1$. Moreover the symmetry of the system implies that the stored energy is defined for minimal representations [55]. Following the approach in Sec. 2, the stored energy is given by the quadratic form generated by the matrix that multiples s (temporal derivative). However, the frequency dependence of $\mathbf{L}$ and $\mathbf{C}_i$ cannot be neglected for finite sized antennas. Moreover, the matrices $\mathbf{L}$ and $\mathbf{C}_i$ have an imaginary part for $\omega > 0$, see App. B. To resolve the issue of frequency dependence, we use differentiation with respect to s of the state-space model to estimate the term that is proportional to s. This expresses the time average stored energy as

$$W_{\widetilde{\mathbf{x}}'} = \frac{1}{4}\widetilde{\mathbf{I}}^H\frac{\partial\widetilde{\mathbf{X}}}{\partial\omega}\widetilde{\mathbf{I}} = \frac{\text{Re}}{4}\begin{pmatrix} \mathbf{I} \\ \mathbf{U} \end{pmatrix}^H\begin{pmatrix} \mu_0(\mathbf{L}+\omega\mathbf{L}') & \mathbf{0} \\ \mathbf{0} & \epsilon_0(\mathbf{C}+\omega\mathbf{C}') \end{pmatrix}\begin{pmatrix} \mathbf{I} \\ \mathbf{U} \end{pmatrix}$$

$$= \frac{\text{Re}}{4}\big(\mu_0\mathbf{I}^H(\mathbf{L}+\omega\mathbf{L}')\mathbf{I} + \epsilon_0\mathbf{U}^H(\mathbf{C}+\omega\mathbf{C}')\mathbf{U}\big)$$

$$\simeq \frac{\text{Re}}{4}\mathbf{I}^H\big(\mu_0(\mathbf{L}+\omega\mathbf{L}') + \frac{1}{\omega^2\epsilon_0}(\mathbf{C}_i-\omega\mathbf{C}_i')\big)\mathbf{I} = \frac{1}{4}\mathbf{I}^H\frac{\partial\mathbf{X}}{\partial\omega}\mathbf{I}, \tag{3.7}$$

where $\mathbf{C}' = -\mathbf{C}\mathbf{C}_i'\mathbf{C}$ is used and the differentiated matrices have the entries

$$L'_{mn} = \frac{\partial L_{mn}}{\partial\omega} = -j\frac{\partial k}{\partial\omega}\int_{\partial\Omega}\int_{\partial\Omega}\boldsymbol{\psi}_m(\boldsymbol{r}_1)\cdot\boldsymbol{\psi}_n(\boldsymbol{r}_2)\frac{e^{-jkR_{12}}}{4\pi}\,dS_1\,dS_2, \tag{3.8}$$

and

$$C'_{imn} = \frac{\partial C_{imn}}{\partial\omega} = -j\frac{\partial k}{\partial\omega}\int_{\partial\Omega}\int_{\partial\Omega}\nabla_1\cdot\boldsymbol{\psi}_m(\boldsymbol{r}_1)\nabla_2\cdot\boldsymbol{\psi}_n(\boldsymbol{r}_2)\frac{e^{-jkR_{12}}}{4\pi}\,dS_1\,dS_2. \tag{3.9}$$

The use of frequency differentiation is an approximation to handle the frequency dependence of $\mathbf{L}$ and $\mathbf{C}_i$. The stored energy (3.7) is dominated by the contribution from $\mathbf{L}$ and $\mathbf{C}_i$ for small antennas [22] and the contributions from $\mathbf{L}'$ and $\mathbf{C}_i'$ are lower order corrections. The $\simeq$ in (3.7) is used to indicate that we neglect the low order correction term $\text{Re}\{\mathbf{I}^H(\mathbf{1}-\mathbf{C}_i^*\mathbf{C}_i^{-1})\mathbf{C}_i'\mathbf{I}\} \approx 0$. These terms are neglected in the remainder of this paper.

The expression (3.7) for the stored energy is identical to the expressions proposed by Harrington and Mautz [31], and Vandenbosch [49] which is equal to the stored energy W_F in (2.2) for the cases where (2.2) is coordinate independent [22]. The stored electric and magnetic energies, and Q-factor are determined as for the circuit network case in (2.9) to (2.11). The time average dissipated power is determined from the Poynting vector and can be expressed as the quadratic form [19, 22, 49] $P_d = \frac{1}{2}\text{Re}\{\mathbf{I}^H\mathbf{V}\} = \frac{1}{2}\mathbf{I}^H\mathbf{RI}$. The stored energy expression (3.7) is compared with the stored energy determined from Brune synthesized circuit models in [21], see also [12, 13, 24, 32]. The results agree very well for antenna sizes up to approximately half-a-wavelength and Q-factors above 5. The problems with larger antennas are caused by the frequency dependence of the matrices $\mathbf{L}$ (3.2) and $\mathbf{C}_i$ (3.3). This frequency dependence implies that (3.5) is not a first order state-space model, hence, the frequency differentiation in (3.7) is only an approximation. This interpretation is analogous to

the difficulties to define the radiated energy in (2.2) and (2.3) for larger antenna structures and originates in the wave nature of the electromagnetic fields that causes phase, or equivalently time, shifts. The state-space approach suggest a possible remedy using rational approximations of the Green's function in (3.2) and (3.3). The problem with the frequency dependence of $\mathbf{L}$ and $\mathbf{C}_i$ is, however, negligible for small antennas with $Q \gg 1$ that are the main focus of this paper.

4 Stored energy for temporally dispersive background media

The classical approach to define stored energy by subtraction of the far-field (2.2) is difficult to generalize to lossy background materials as the far-field vanishes. This implies that W_F equals the total energy in a lossy background and that $W_F \to \infty$ as the losses approach zero. Here, we use the state-space approach to generalize the expressions for the stored energy in Sec. 3 to background materials with losses and temporally dispersive permittivity in Sec. 4.1, and combined permittivity and permeability in Sec. 4.2.

4.1 Temporally dispersive permittivity

The MoM impedance matrix in temporally dispersive media is formally identical to the free space case (3.1) with the use of the complex-valued wavenumber k in the background medium. Consider for simplicity a non-magnetic media with the permittivity described by a single Lorentz resonance [4, 33]

$$\epsilon(s) = \epsilon_\infty + \frac{\alpha^2}{\beta^2 + \gamma s + \delta s^2} = \epsilon_\infty + \frac{\alpha^2}{\chi}, \tag{4.1}$$

where ϵ_∞ is the instantaneous response, $\alpha, \beta, \gamma, \delta$ are the Lorentz parameters, and χ is introduced for notational simplicity. This model reduces to conductivity, Debye, and Drude models with specific parameter choices and is easily extended to multiple resonances. The system (3.5) is rewritten to a first order system by introduction of the voltage state $\mathbf{U}$, polarization state $\mathbf{P}$, and its temporal derivative $\dot{\mathbf{P}} = \beta^{-1} s \mathbf{P}$, i.e.,

$$\mathbf{I} = s\epsilon \mathbf{CU} = \left(s\epsilon_\infty + \frac{s\alpha^2}{\beta^2 + \gamma s + \delta s^2}\right)\mathbf{CU} = s\epsilon_\infty \mathbf{CU} + \alpha\dot{\mathbf{P}}, \tag{4.2}$$

where $\mathbf{C} = \mathbf{C}_i^{-1}$ is used for simplicity. Note that $\mathbf{C}_i$ has a null space and is not invertible. This is resolved in the final expressions for the stored energy below. The rational and second order s-term in $\alpha\dot{\mathbf{P}}$ are removed by multiplication with $\chi\mathbf{C}_i/(s\alpha)$, i.e.,

$$\alpha\mathbf{U} = (\beta^2 + \gamma s + \delta s^2)\frac{1}{s}\mathbf{C}_i\dot{\mathbf{P}} = \beta\mathbf{C}_i\mathbf{P} + (\gamma + \delta s)\mathbf{C}_i\dot{\mathbf{P}}. \tag{4.3}$$

Collecting the equations (3.5), (4.2), $s\mathbf{C}_i\mathbf{P} = \beta\mathbf{C}_i\dot{\mathbf{P}}$, and (4.3) gives the linear system

$$\widetilde{\mathbf{Z}}\widetilde{\mathbf{I}} = \begin{pmatrix} s\mu\mathbf{L} & \mathbf{1} & \mathbf{0} & \mathbf{0} \\ -\mathbf{1} & s\epsilon_\infty\mathbf{C} & \mathbf{0} & \mathbf{1}\alpha \\ \mathbf{0} & \mathbf{0} & s\mathbf{C}_i & -\beta\mathbf{C}_i \\ \mathbf{0} & -\mathbf{1}\alpha & \beta\mathbf{C}_i & (s\delta + \gamma)\mathbf{C}_i \end{pmatrix} \begin{pmatrix} \mathbf{I} \\ \mathbf{U} \\ \mathbf{P} \\ \dot{\mathbf{P}} \end{pmatrix} = \begin{pmatrix} \mathbf{V} \\ \mathbf{0} \\ \mathbf{0} \\ \mathbf{0} \end{pmatrix} = \widetilde{\mathbf{B}}V_{\text{in}}, \tag{4.4}$$

with the output $I_{\text{in}} = \mathbf{B}^{\text{T}}\mathbf{I} = \widetilde{\mathbf{B}}^{\text{T}}\widetilde{\mathbf{I}}$, and input V_{in}. This is a classical state-space representation [55] in the limit of small antennas, where the s-dependence of the matrices $\mathbf{L}$ and $\mathbf{C}_i$ is negligible. Furthermore, the representation is reciprocal with internal symmetry $\text{diag}(\mathbf{1}, -\mathbf{1}, -\mathbf{1}, \mathbf{1})$, see [55].

To calculate the stored energy of the system (4.4), the term proportional to s is estimated by differentiation with respect to s

$$\frac{\partial\widetilde{\mathbf{Z}}}{\partial s} = \begin{pmatrix} \mu\mathbf{L} + \omega\mu\mathbf{L}' & \mathbf{0} & \mathbf{0} & \mathbf{0} \\ \mathbf{0} & \epsilon_\infty\mathbf{C} + \omega\epsilon_\infty\mathbf{C}' & \mathbf{0} & \mathbf{0} \\ \mathbf{0} & \mathbf{0} & \mathbf{C}_i + \omega\mathbf{C}_i' & j\beta\mathbf{C}_i' \\ \mathbf{0} & \mathbf{0} & -j\beta\mathbf{C}_i' & \delta\mathbf{C}_i + (\omega\delta - j\gamma)\mathbf{C}_i' \end{pmatrix}, \tag{4.5}$$

where frequency dependence of the matrices $\mathbf{L}$ and $\mathbf{C}_i$ are approximated locally using frequency differentiation [26]. The stored energy is finally calculated by the quadratic form obtained by multiplication of (4.5) with the states from the left and right. A closed form expressions is derived by back substitution of the explicit expressions of the states expressed in the current $\mathbf{I}$. Use that $\mathbf{CU} = \frac{1}{s\epsilon}\mathbf{I}$, $\dot{\mathbf{P}} = \frac{s}{\beta}\mathbf{P}$, $\mathbf{P} = \frac{\alpha\beta}{s\epsilon\chi}\mathbf{I}$, and

$$\beta\left(-\mathbf{P}^H\mathbf{C}_i'\dot{\mathbf{P}} + \dot{\mathbf{P}}^H\mathbf{C}_i'\mathbf{P}\right) = \left(-j\omega\mathbf{P}^H\mathbf{C}_i'\mathbf{P} - j\omega\mathbf{P}^H\mathbf{C}_i'\mathbf{P}\right) = -2j\omega\mathbf{P}^H\mathbf{C}_i'\mathbf{P}$$

to express the stored energy as

$$W_{\widetilde{\mathbf{X}}'} = \frac{\mathrm{Re}}{4}\mathbf{I}^H\left(\mu\mathbf{L} + \frac{\epsilon_\infty}{|\omega\epsilon|^2}\mathbf{C}_i + \omega\mu\mathbf{L}' - \frac{\omega\epsilon_\infty}{|\omega\epsilon|^2}\mathbf{C}_i'\right)\mathbf{I}$$
$$+ \frac{\mathrm{Re}}{4}\mathbf{P}^H\left(\mathbf{C}_i + \mathbf{C}_i\delta\frac{\omega^2}{\beta^2} + \omega\mathbf{C}_i' + \omega^2\frac{\omega\delta - j\gamma}{\beta^2}\mathbf{C}_i' - 2\omega\mathbf{C}_i'\right)\mathbf{P}, \quad (4.6)$$

where the low-order term in (3.7) is neglected. The second part multiplying $\mathbf{P}$ can be written as

$$(\beta^2 + \delta\omega^2)\mathbf{C}_i - \omega(\beta^2 - \omega^2\delta + j\omega\gamma)\mathbf{C}_i' = (\beta^2 + \delta\omega^2)\mathbf{C}_i - \omega\chi\mathbf{C}_i', \quad (4.7)$$

that together with elimination of $\mathbf{P}$ express the stored energy as the quadratic form

$$W_{\widetilde{\mathbf{X}}'} = \frac{\mathrm{Re}}{4}\mathbf{I}^H\left(\mu\mathbf{L} + \frac{\epsilon_\infty}{|\omega\epsilon|^2}\mathbf{C}_i + \omega\mu\mathbf{L}' - \frac{\omega\epsilon_\infty}{|\omega\epsilon|^2}\mathbf{C}_i' + \frac{\alpha^2\left((\beta^2 + \omega^2\delta)\mathbf{C}_i - \omega\chi\mathbf{C}_i'\right)}{|\omega\epsilon|^2|\chi|^2}\right)\mathbf{I} \quad (4.8)$$

in the current $\mathbf{I}$. The solution simplifies for the reduced models, e.g., the conductivity model $\epsilon = \epsilon_\infty + \sigma/s$ with $\alpha^2/\gamma = \sigma$, $\beta = \delta = 0$, and $\chi = s\gamma$ has the stored energy

$$W_{\widetilde{\mathbf{X}}'} = \frac{\mathrm{Re}}{4}\mathbf{I}^H\left(\mu\mathbf{L} + \frac{\epsilon_\infty}{\omega^2\epsilon_\infty^2 + \sigma^2}\mathbf{C}_i + \omega\mu\mathbf{L}' - \frac{j\sigma + \omega\epsilon_\infty}{\omega^2\epsilon_\infty^2 + \sigma^2}\mathbf{C}_i'\right)\mathbf{I}. \quad (4.9)$$

It is also straight forward to generalize the stored energy expressions to multiple resonances.

We follow (2.9), (2.10), and (2.11) to determine the stored electric and magnetic energies and Q-factor for the state-space model. The frequency derivative of the state-space matrix $\widetilde{\mathbf{X}}'$ produces the quadratic forms for the stored energies in (3.7), i.e.,

$$W_{\widetilde{\mathbf{X}}'} = W_{e\widetilde{\mathbf{X}}'} + W_{m\widetilde{\mathbf{X}}'} = \frac{1}{4}\widetilde{\mathbf{I}}^H\frac{\partial\widetilde{\mathbf{X}}}{\partial\omega}\widetilde{\mathbf{I}} = \frac{1}{4\omega}\mathbf{I}^H(\mathbf{X}_e + \mathbf{X}_m)\mathbf{I}, \quad (4.10)$$

where (4.8) is used to introduce the electric, $\mathbf{X}_e$, and magnetic, $\mathbf{X}_m$, reactance matrices for dispersive media [23, 24]. The difference between the stored magnetic and electric energies give the explicit formulas for the stored magnetic and electric energies

$$W_{m\widetilde{\mathbf{X}}'} = \frac{1}{8}\widetilde{\mathbf{I}}^H\left(\frac{\partial\widetilde{\mathbf{X}}}{\partial\omega} + \frac{\widetilde{\mathbf{X}}}{\omega}\right)\widetilde{\mathbf{I}} = \frac{1}{4\omega}\mathbf{I}^H\mathbf{X}_m\mathbf{I} \quad (4.11)$$

and

$$W_{e\widetilde{\mathbf{X}}'} = \frac{1}{8}\widetilde{\mathbf{I}}^H\left(\frac{\partial\widetilde{\mathbf{X}}}{\partial\omega} - \frac{\widetilde{\mathbf{X}}}{\omega}\right)\widetilde{\mathbf{I}} = \frac{1}{4\omega}\mathbf{I}^H\mathbf{X}_e\mathbf{I}, \quad (4.12)$$

respectively. The relations (4.11) and (4.12) are formally identical to the stored energy expressions for the lumped circuit networks (2.9) and (2.10). The Q-factor for antennas tuned to resonance (2.1) is

$$Q_{\widetilde{\mathbf{X}}'} = \frac{\max\{\widetilde{\mathbf{I}}^H(\omega\widetilde{\mathbf{X}}' \pm \widetilde{\mathbf{X}})\widetilde{\mathbf{I}}\}}{2\mathbf{I}^H\mathbf{R}\mathbf{I}} = \frac{\omega\widetilde{\mathbf{I}}^H\widetilde{\mathbf{X}}'\widetilde{\mathbf{I}} + |\mathbf{I}^H\mathbf{X}\mathbf{I}|}{2\mathbf{I}^H\mathbf{R}\mathbf{I}} = \frac{\max\{\mathbf{I}^H\mathbf{X}_e\mathbf{I}, \mathbf{I}^H\mathbf{X}_m\mathbf{I}\}}{\mathbf{I}^H\mathbf{R}\mathbf{I}} \quad (4.13)$$
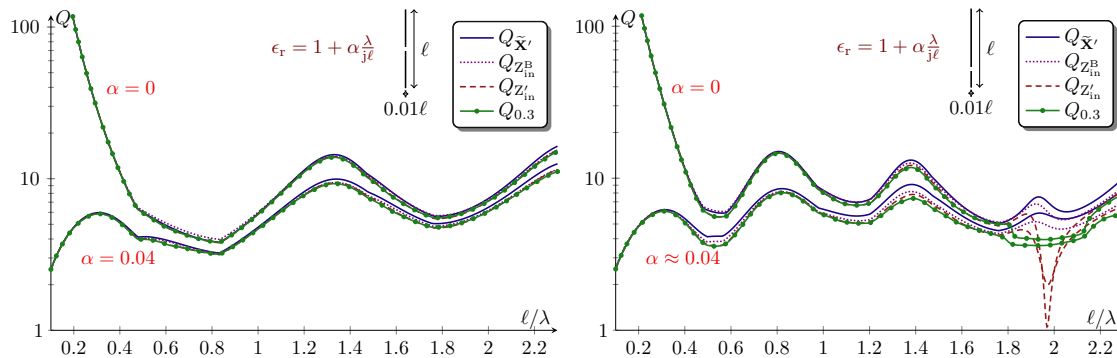
for the stored energy (4.10).

Figure 3: Q-factors for strip dipoles with length ℓ, width $\ell/100$, and fed in the center and 0.27ℓ from the center to the left and right, respectively. The antennas are placed in a homogeneous medium with relative permittivity $\epsilon_{\mathrm{r}} = 1 - \alpha\mathrm{j}/\omega$, where $\omega = 2\pi\ell/\lambda$. The Q-factors are determined from the state-space matrix $Q_{\widetilde{\mathbf{X}}'}$ in (4.13), the Brune synthesized circuit model $Q_{Z_{\mathrm{in}}^{\mathrm{B}}}$ as in [21], the differentiated input impedance $Q_{Z'_{\mathrm{in}}}$ in (A.1), and fractional bandwidth $Q_{0.3}$ (A.3) with $\Gamma_0 = 0.3$.

We compare the Q-factor determined from the state-space model $Q_{\widetilde{\mathbf{X}}'}$ using (4.8) with the differentiated input impedance $Q_{Z'_{\mathrm{in}}}$ (A.1), Brune synthesis $Q_{Z_{\mathrm{in}}^{\mathrm{B}}}$ [21], and $\Gamma_0 = 0.3$ reflection coefficient $Q_{0.3}$ (A.3) in Figs. 3, 4, and 5. The antenna parameters are computed using a MoM code based on rectangular elements for planar (negligible thickness) structures modeled as PECs. We consider non-dispersive, conductivity, and Lorentz permittivity models for dipole antennas with length ℓ and width 0.01ℓ in Figs 3 and 4. The results are presented in the dimensionless parameter ℓ/λ, where λ is the free space wavelength. The material parameters are functions of the dimensionless parameter $\omega = 2\pi\ell/\lambda$.

Fig. 3 depicts strip dipoles, fed at the center and 0.27ℓ from the center, in a homogenous medium with relative permittivity $\epsilon_{\mathrm{r}} = 1 - \mathrm{j}\sigma/\omega$. The off-center feed is chosen to eliminate some of the symmetries of the induced current density distribution in comparison to the center-fed case, and increase the phase shift of the induced current density. The calculated Q-factors are depicted in Fig. 3 for free space and background media with relative permittivity $\epsilon_{\mathrm{r}} = 1 - \mathrm{j}0.25/\omega \approx 1 - \mathrm{j}0.04\lambda/\ell$. All Q-factors seem to agree well for the center fed dipole in the left hand figure. For the off-center fed dipole in the right hand figure the Q-factors agree well for low frequencies, but tend to deviate slightly at higher frequencies. At low frequencies the loss tangent $0.25/\omega$ is high and thus all Q-factors are small. The Q-factor from the Brune circuit $Q_{Z_{\mathrm{in}}^{\mathrm{B}}}$ follow $Q_{\widetilde{\mathbf{X}}'}$, but gives slightly lower values. The Q-factor from the differentiated input impedance $Q_{Z'_{\mathrm{in}}}$ is similar to $Q_{Z_{\mathrm{in}}^{\mathrm{B}}}$ except for $\ell/\lambda \approx 2$ in the off-center fed case, where $Q_{Z'_{\mathrm{in}}}$ has a dip. This dip is mimicked in the free space case where $Q_{Z'_{\mathrm{in}}} \approx 0$, see also [21]. $Q_{0.3}$ also deviates from $Q_{\widetilde{\mathbf{X}}'}$ at $\ell/\lambda \approx 2$ where it has a fixed lower level. $Q_{\widetilde{\mathbf{X}}'}$ and $Q_{Z_{\mathrm{in}}^{\mathrm{B}}}$ do not seem to be affected by these effects and predict values of around 7 in this region.

Fig. 4 shows the Q-factors for a center fed dipole in a background Lorentz media. The background has been modeled by the Lorentz model

$$\epsilon_{\mathrm{r}} = 1 + \frac{\nu^2\omega_0^2/2}{\omega_0^2 + s\nu\omega_0 + s^2}, \tag{4.14}$$

with the values

$$\epsilon_{\mathrm{r}}(\omega_0) = 1 - \mathrm{j}\nu/4 \quad \text{and} \quad (\omega\epsilon_{\mathrm{r}})'|_{\omega=\omega_0} = 0, \tag{4.15}$$

where ω_0 is the resonance frequency of the material. All Q-factors agree well outside the resonance $\omega_0 \approx 0.25$. The state-space model $Q_{\widetilde{\mathbf{X}}'}$ and Brune circuit $Q_{Z_{\mathrm{in}}^{\mathrm{B}}}$ are similar at ω_0, whereas $Q_{Z'_{\mathrm{in}}}$ and $Q_{0.3}$ are lower. The similarities between $Q_{\widetilde{\mathbf{X}}'}$ and $Q_{Z_{\mathrm{in}}^{\mathrm{B}}}$ indicate that (4.8) is accurate for small antennas in highly dispersive backgrounds. The lower values for $Q_{Z'_{\mathrm{in}}}$ show that Z_{in} is not well
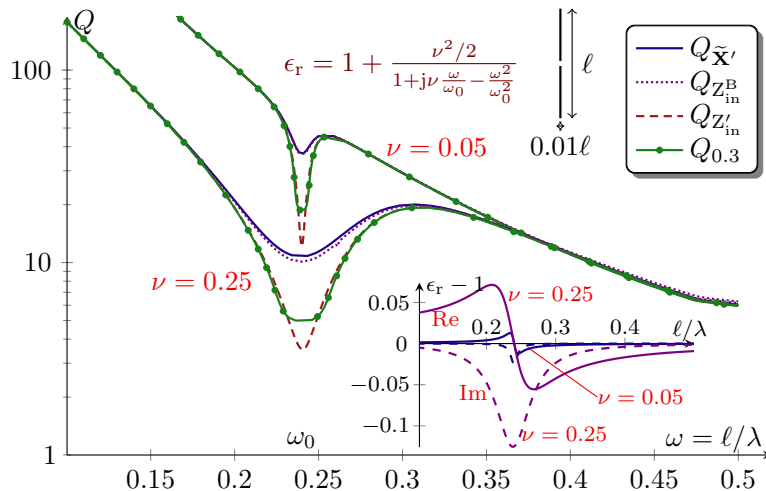
Figure 4: Q-factors for a center fed strip dipole with length ℓ, and width $\ell/100$, placed in a homogeneous medium with relative permittivity (4.14), where $\omega = 2\pi\ell/\lambda$ and $\nu = \{0.25, 0.05\}$. The permittivity is depicted in the bottom right. The Q-factors are determined from the state-space matrix $Q_{\widetilde{\mathbf{X}}'}$ in (4.13), the Brune synthesized circuit model $Q_{Z_{\text{in}}^{\text{B}}}$ as in [21], the differentiated input impedance $Q_{Z_{\text{in}}'}$ in (A.1), and fractional bandwidth $Q_{0.3}$ (A.3) with $\Gamma_0 = 0.3$.

approximated with a single resonances model around ω_0. The fractional bandwidth $Q_{0.3}$ agrees with $Q_{Z_{\text{in}}'}$ as $\Gamma_0 \to 0$, but is closer to $Q_{Z_{\text{in}}^{\text{B}}}$ for larger values of Γ_0.

Fig. 5 depicts the Q-factors for a meander line antenna following the design in [3]. The Q-factors have been calculated for an intervall around the operating frequency of the antenna and seem to agree well with $Q_{Z_{\text{in}}^{\text{B}}}$ and $Q_{Z_{\text{in}}'}$ predicting slightly lower values than $Q_{\widetilde{\mathbf{X}}'}$ for greater losses. This illustrates the state-space methods ability to also accurately calculate the Q-factor for more advanced antenna structures.

4.2 Temporally dispersive permittivity and permeability

Temporally dispersive permittivity and permeability are used to model metamaterials and can produce exotic phenomena such as negative refraction [1, 2, 9]. These are very challenging material models and good cases to verify the accuracy of the stored energy expressions [28]. Here, the state-space model is generalized to Lorentz models in the permittivity and permeability, *i.e.*,

$$\epsilon(s) = \epsilon_\infty + \frac{\alpha^2}{\beta^2 + \gamma s + \delta s^2} \quad \text{and} \quad \mu(s) = \mu_\infty + \frac{\alpha_1^2}{\beta_1^2 + \gamma_1 s + \delta_1 s^2}, \tag{4.16}$$

where the parameters are defined in analogy to (4.1), and are assumed to be non-negative. Following the approach in Sec. 4.1, we introduce the voltage state $\mathbf{U}$, electric polarizability $\mathbf{P}$ and $\dot{\mathbf{P}}$, and the magnetic polarizability $\mathbf{P}_{\text{m}}$ and $\dot{\mathbf{P}}_{\text{m}}$. The EFIE MoM system is rewritten,

$$\mathbf{ZI} = (s\mu\mathbf{L} + \frac{1}{s\epsilon}\mathbf{C}_{\text{i}})\mathbf{I} = s\mu_\infty\mathbf{LI} + \alpha_1\dot{\mathbf{P}}_{\text{m}} + \mathbf{U} = \mathbf{V} = \mathbf{B}V_{\text{in}}, \tag{4.17}$$

with the magnetic polarizability $\dot{\mathbf{P}}_{\text{m}} = \frac{s\alpha_1}{\beta_1^2 + \gamma_1 s + \delta_1 s^2}\mathbf{LI}$. The equation is divided into its electric and magnetic parts relating to the permittivity and permeability, respectively. The electric part is identical to (4.2) and analyzed as in Sec. 4.1. The magnetic part is similarly rewritten using

$$\alpha_1\mathbf{LI} = (\frac{\beta_1^2}{s} + \gamma_1 + \delta_1 s)\dot{\mathbf{P}}_{\text{m}} = \beta_1\mathbf{P}_{\text{m}} + \gamma_1\dot{\mathbf{P}}_{\text{m}} + \delta_1 s\dot{\mathbf{P}}_{\text{m}}. \tag{4.18}$$

Figure 5: Q-factors for meander line antenna 'M1' in [3], with height ℓ, width 0.56ℓ, and placed in a homogeneous Debye medium with relative permittivity (4.1). The Lorentz parameters are chosen as $\alpha = \{0.2, 0.4, 0.6, 0.8, 1.0\}, \beta = 1, \gamma = 4, \delta = 0$ (♠). The antenna geometry is depicted in the upper right hand corner as well as the permittivity over the frequency interval. The Q-factor has been calculated with the state-space model $Q_{\widetilde{\mathbf{X}}'}$, Brune synthesis $Q_{Z_{\mathrm{in}}^{\mathrm{B}}}$, and differentiation of the impedance matrix $Q_{Z'_{\mathrm{in}}}$.

Collecting the terms gives the state-space model

$$
\begin{pmatrix}
s\mu_\infty\mathbf{L} & \mathbf{1} & \mathbf{0} & \mathbf{0} & \mathbf{0} & \alpha_1\mathbf{1} \\
-\mathbf{1} & s\epsilon_\infty\mathbf{C} & \mathbf{0} & \mathbf{1}\alpha & \mathbf{0} & \mathbf{0} \\
\mathbf{0} & \mathbf{0} & s\mathbf{C}_\mathrm{i} & -\beta\mathbf{C}_\mathrm{i} & \mathbf{0} & \mathbf{0} \\
\mathbf{0} & -\alpha\mathbf{1} & \beta\mathbf{C}_\mathrm{i} & (s\delta+\gamma)\mathbf{C}_\mathrm{i} & \mathbf{0} & \mathbf{0} \\
\mathbf{0} & \mathbf{0} & \mathbf{0} & \mathbf{0} & s\mathbf{L}^{-1} & -\beta_1\mathbf{L}^{-1} \\
-\alpha_1\mathbf{1} & \mathbf{0} & \mathbf{0} & \mathbf{0} & \beta_1\mathbf{L}^{-1} & (s\delta_1+\gamma_1)\mathbf{L}^{-1}
\end{pmatrix}
\begin{pmatrix}
\mathbf{I} \\ \mathbf{U} \\ \mathbf{P} \\ \dot{\mathbf{P}} \\ \mathbf{P}_\mathrm{m} \\ \dot{\mathbf{P}}_\mathrm{m}
\end{pmatrix}
=
\begin{pmatrix}
\mathbf{B} \\ \mathbf{0} \\ \mathbf{0} \\ \mathbf{0} \\ \mathbf{0} \\ \mathbf{0}
\end{pmatrix}
V_{\mathrm{in}}. \qquad (4.19)
$$

The stored energy is approximated as the quadratic form generated by the differentiated system matrix in (4.19),

$$
\begin{pmatrix}
\mu_\infty\mathbf{L}+\omega\mu_\infty\mathbf{L}' & \mathbf{0} & \mathbf{0} & \mathbf{0} & \mathbf{0} & \mathbf{0} \\
\mathbf{0} & \epsilon_\infty\mathbf{C}+\omega\epsilon_\infty\mathbf{C}' & \mathbf{0} & \mathbf{0} & \mathbf{0} & \mathbf{0} \\
\mathbf{0} & \mathbf{0} & \mathbf{C}_\mathrm{i}+\omega\mathbf{C}_\mathrm{i}' & \mathrm{j}\beta\mathbf{C}_\mathrm{i}' & \mathbf{0} & \mathbf{0} \\
\mathbf{0} & \mathbf{0} & -\mathrm{j}\beta\mathbf{C}_\mathrm{i}' & \delta\mathbf{C}_\mathrm{i}+(\omega\delta-\mathrm{j}\gamma)\mathbf{C}_\mathrm{i}' & \mathbf{0} & \mathbf{0} \\
\mathbf{0} & \mathbf{0} & \mathbf{0} & \mathbf{0} & \mathbf{L}_\mathrm{i}+\omega\mathbf{L}_\mathrm{i}' & \mathrm{j}\beta_1\mathbf{L}_\mathrm{i}' \\
\mathbf{0} & \mathbf{0} & \mathbf{0} & \mathbf{0} & -\mathrm{j}\beta_1\mathbf{L}_\mathrm{i}' & \delta_1\mathbf{L}_\mathrm{i}+(\omega\delta_1-\mathrm{j}\gamma_1)\mathbf{L}_\mathrm{i}'
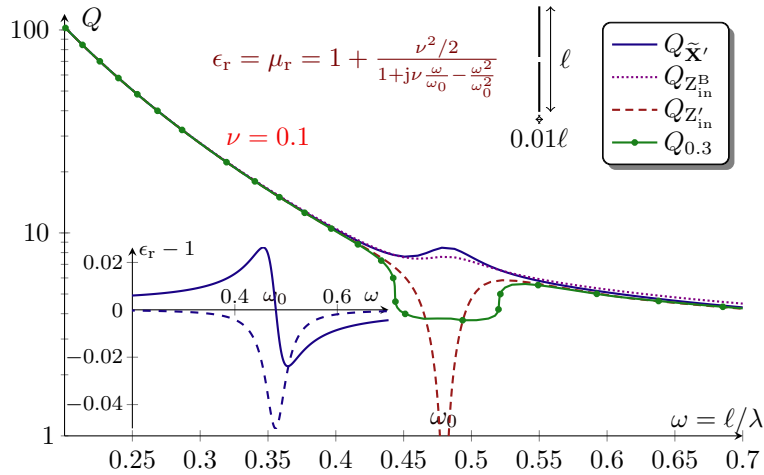\end{pmatrix}.
$$

Figure 6: Q-factors for a strip dipole with length ℓ, width $\ell/100$, fed at the center, and placed in a homogeneous electric and magnetic Lorentz medium with relative permittivity and permeability (4.16) as depicted in the bottom left inset, where $\omega = 2\pi\ell/\lambda$ and $\nu = 10^{-1}$. The Q-factors are determined from the state-space matrix $Q_{\widetilde{\mathbf{X}}'}$, the Brune synthesized circuit model $Q_{Z_{\text{in}}^{\text{B}}}$, the differentiated input impedance $Q_{Z_{\text{in}}'}$, and fractional bandwidth $Q_{0.3}$.

The electric terms are analyzed in Sec. 4.1 and the magnetic terms are similarly simplified as

$$
\begin{pmatrix} \mathbf{P}_{\text{m}} \\ \dot{\mathbf{P}}_{\text{m}} \end{pmatrix}^{\text{H}} \begin{pmatrix} \mathbf{L}^{-1} - \omega\mathbf{L}^{-1}\mathbf{L}'\mathbf{L}^{-1} & -\mathrm{j}\beta_1\mathbf{L}^{-1}\mathbf{L}'\mathbf{L}^{-1} \\ \mathrm{j}\beta_1\mathbf{L}^{-1}\mathbf{L}'\mathbf{L}^{-1} & \delta_1\mathbf{L}^{-1} - (\omega\delta_1 - \mathrm{j}\gamma_1)\mathbf{L}^{-1}\mathbf{L}'\mathbf{L}^{-1} \end{pmatrix} \begin{pmatrix} \mathbf{P}_{\text{m}} \\ \dot{\mathbf{P}}_{\text{m}} \end{pmatrix}
$$

$$
= \begin{pmatrix} \frac{\alpha_1\beta_1}{\chi_1}\mathbf{L}\mathbf{I} \\ \frac{\alpha_1 s}{\chi_1}\mathbf{L}\mathbf{I} \end{pmatrix}^{\text{H}} \begin{pmatrix} \mathbf{L}^{-1} - \omega\mathbf{L}^{-1}\mathbf{L}'\mathbf{L}^{-1} & -\mathrm{j}\beta_1\mathbf{L}^{-1}\mathbf{L}'\mathbf{L}^{-1} \\ \mathrm{j}\beta_1\mathbf{L}^{-1}\mathbf{L}'\mathbf{L}^{-1} & \delta_1\mathbf{L}^{-1} - (\omega\delta_1 - \mathrm{j}\gamma_1)\mathbf{L}^{-1}\mathbf{L}'\mathbf{L}^{-1} \end{pmatrix} \begin{pmatrix} \frac{\alpha_1\beta_1}{\chi_1}\mathbf{L}\mathbf{I} \\ \frac{\alpha_1 s}{\chi_1}\mathbf{L}\mathbf{I} \end{pmatrix}
$$

$$
\simeq \begin{pmatrix} \frac{\alpha_1\beta_1}{\chi_1}\mathbf{I} \\ \frac{\alpha_1 s}{\chi_1}\mathbf{I} \end{pmatrix}^{\text{H}} \begin{pmatrix} \mathbf{L} - \omega\mathbf{L}' & -\mathrm{j}\beta_1\mathbf{L}' \\ \mathrm{j}\beta_1\mathbf{L}' & \delta_1\mathbf{L} - (\omega\delta_1 - \mathrm{j}\gamma_1)\mathbf{L}' \end{pmatrix} \begin{pmatrix} \frac{\alpha_1\beta_1}{\chi_1}\mathbf{I} \\ \frac{\alpha_1 s}{\chi_1}\mathbf{I} \end{pmatrix}
$$

$$
= \frac{\alpha_1^2}{|\chi_1^2|}\mathbf{I}^{\text{H}}\big(\beta_1^2(\mathbf{L} - \omega\mathbf{L}') + 2\omega\beta_1^2\mathbf{L}' + \omega^2(\delta_1\mathbf{L} - (\omega\delta_1 - \mathrm{j}\gamma_1)\mathbf{L}')\big)\mathbf{I}
$$

$$
= \frac{\alpha_1^2}{|\chi_1^2|}\mathbf{I}^{\text{H}}\big((\beta_1^2 + \omega^2\delta_1)\mathbf{L} + \omega(\beta_1^2 - \omega^2\delta_1 + \mathrm{j}\omega\gamma_1)\mathbf{L}')\big)\mathbf{I} = \frac{\alpha_1^2}{|\chi_1^2|}\mathbf{I}^{\text{H}}\big((\beta_1^2 + \omega^2\delta_1)\mathbf{L} + \omega\chi_1\mathbf{L}'\big)\mathbf{I}, \quad (4.20)
$$

where we again neglect the lower order terms.

If we consider a medium with permittivity and permeability according to the Lorentz model (4.16) and $\mu_{\text{r}} = \epsilon_{\text{r}}$. This synthesizes a case where $\mathbf{Z}' \approx \mathbf{0}$ for antennas that are resonant at ω_0 [28] for any $\nu > 0$. Furthermore, the corresponding impedance matrix does not change significantly as $\nu \to 0$, i.e., $\mathbf{Z}_\nu \approx \mathbf{Z}_{\nu=0}$ as $\nu \ll 1$. Therefore, the energy distribution in the fields, currents, or circuit models of the antenna depend weakly on ν as $\nu \ll 1$.

In Fig. 6 a strip dipole with length ℓ and width 0.01ℓ are used to illustrate the estimated Q-factors. Consider the resonance frequency $\omega_0 = 2\pi\ell/\lambda = 3$ and the damping $\nu = 0.1$ in the Lorentz model (4.16). The maximal susceptibility is $|1 - \epsilon_{\text{r}}| = \nu/\sqrt{4 - \nu^2} \approx \nu/2$ for $\nu \ll 1$. The Q-factors give similar results away from the resonance frequency ω_0, which coincides with the dipole resonance of the antenna. At ω_0 $Q_{Z_{\text{in}}'}$ has a substantial dip, whereas $Q_{\widetilde{\mathbf{X}}'}$ and $Q_{Z_{\text{in}}^{\text{B}}}$ increase slightly. $Q_{Z_{\text{in}}^{\text{B}}}$ has slightly lower values than $Q_{\widetilde{\mathbf{X}}'}$ at the resonance ω_0. $Q_{0.3}$ on the other hand also displays a bottoming out of its values around the resonance, cf., with [28]. This in conjunction with $Q_{Z_{\text{in}}'}$ behavior indicate that the single resonance approximation for Z_{in} is not satisfied in this kind of resonant media.

5 Stored energy for inhomogeneous media

The numerical examples in Sec. 4 indicate that the state-space approach produces accurate estimates of the stored energy for homogeneous background media. Following this approach, we analyze piecewise homogeneous background media using the surface equivalence principle, and inhomogeneous media with volume integral equations in Secs 5.1 and 5.2, respectively.

5.1 Piecewise homogeneous media

The surface equivalence principle is used to express the electromagnetic fields in piecewise homogeneous media [4, 10, 35, 44, 52]. Consider for simplicity a PEC antenna structure embedded in a media with permittivity and permeability as depicted in Fig. 2. The geometry is divided into three regions Ω_p $p = 1, 2, 3$, with corresponding material parameters ϵ_p and μ_p. Let $\partial\Omega_p$ denote the exterior surface of Ω_p, *i.e.*, the boundary of $\bigcup_{q=1}^{p} \Omega_q$. The field in region Ω_p is expressed by the equivalent currents $\boldsymbol{J}_{p-1}, \boldsymbol{J}_p, \boldsymbol{M}_{p-1}$, and $\boldsymbol{M}_p$, where $\boldsymbol{J}_0 = \boldsymbol{M}_0 = \boldsymbol{0}$. We follow the state-space approach and construct a system for the input impedance $Z_{\text{in}} = V_{\text{in}}/I_{\text{in}}$.

The EFIE and magnetic field integral equation (MFIE) for the inner region Ω_2 is written

$$\begin{pmatrix} \mathbf{Z}_{2,11} & \mathbf{Z}_{2,12} & \mathbf{K}_{2,12} \\ \mathbf{Z}_{2,21} & \mathbf{Z}_{2,22} & \mathbf{K}_0 + \mathbf{K}_{2,22} \\ -\mathbf{K}_{2,21} & \mathbf{K}_0 - \mathbf{K}_{2,22} & \frac{1}{\eta_2^2}\mathbf{Z}_{2,22} \end{pmatrix} \begin{pmatrix} \mathbf{I}_1 \\ \mathbf{I}_2 \\ \mathbf{M}_2 \end{pmatrix} = \begin{pmatrix} \mathbf{V}_1 \\ \mathbf{0} \\ \mathbf{0} \end{pmatrix}, \tag{5.1}$$

where $\mathbf{Z}_{p,oq}$ denotes the EFIE impedance matrix (3.1) connecting the surfaces o and q through their respective currents, evaluated using materials ϵ_p and μ_p. $\mathbf{K}_{p,oq}$ is the corresponding MFIE operator with elements

$$K_{p,oq,mn} = \int_{\partial\Omega_o} \int_{\partial\Omega_q} \boldsymbol{\psi}_m(\boldsymbol{r}_1) \cdot \boldsymbol{\psi}_n(\boldsymbol{r}_2) \times \nabla_1 G_{12}\, \mathrm{dS}_1\, \mathrm{dS}_2 \tag{5.2}$$

and $\mathbf{K}_0$ is the free term of the MFIE. Since region 1 is a PEC, there exists no magnetic surface current $\mathbf{M}_1$. The EFIE and MFIE for the exterior region Ω_3 is similarly

$$\begin{pmatrix} \mathbf{Z}_{3,22} & -\mathbf{K}_0 + \mathbf{K}_{3,22} \\ -\mathbf{K}_0 - \mathbf{K}_{3,22} & \frac{1}{\eta_3^2}\mathbf{Z}_{3,22} \end{pmatrix} \begin{pmatrix} \mathbf{I}_2 \\ \mathbf{M}_2 \end{pmatrix} = \begin{pmatrix} \mathbf{0} \\ \mathbf{0} \end{pmatrix}. \tag{5.3}$$

The EFIE and MFIE in (5.1) and (5.3) can be combined in different ways to mitigate internal resonance problems of the MoM solution, *e.g.*, the PMCHWT and Müller integral equations [10, 35]. Here, we choose the PMCHWT formulation and add the equations (5.1) and (5.3) together to get

$$\begin{pmatrix} \mathbf{Z}_{2,11} & \mathbf{Z}_{2,12} & \mathbf{K}_{2,12} \\ \mathbf{Z}_{2,21} & \mathbf{Z}_{2,22} + \mathbf{Z}_{3,22} & \mathbf{K}_{2,22} + \mathbf{K}_{3,22} \\ -\mathbf{K}_{2,21} & -\mathbf{K}_{2,22} - \mathbf{K}_{3,22} & \frac{1}{\eta_2^2}\mathbf{Z}_{2,22} + \frac{1}{\eta_3^2}\mathbf{Z}_{3,22} \end{pmatrix} \begin{pmatrix} \mathbf{I}_1 \\ \mathbf{I}_2 \\ \mathbf{M}_2 \end{pmatrix} = \begin{pmatrix} \mathbf{V}_1 \\ \mathbf{0} \\ \mathbf{0} \end{pmatrix}, \tag{5.4}$$

where the $\mathbf{K}_0$ term cancels out. This can be considered as a second order state-space model for the input impedance with the decomposition (3.1). Because the material parameters are different in the two regions it is, however, advantageous to first divide (5.4) as a sum of its inner and outer parts. This creates two parts that are formally identical and can be written as

$$\begin{pmatrix} \mathbf{Z} & \mathbf{K} \\ -\mathbf{K} & \mathbf{Z} \end{pmatrix} \begin{pmatrix} \mathbf{I} \\ \mathbf{M} \end{pmatrix} = \begin{pmatrix} s\mu\mathbf{L} + \frac{\mathbf{C}_{\mathrm{i}}}{s\epsilon} & \mathbf{K} \\ -\mathbf{K} & s\epsilon\mathbf{L} + \frac{\mathbf{C}_{\mathrm{i}}}{s\mu} \end{pmatrix} \begin{pmatrix} \mathbf{I} \\ \mathbf{M} \end{pmatrix}, \tag{5.5}$$

where the material parameters ϵ_p and μ_p are used in region Ω_p. The second order system (5.5) is rewritten as a first order system, in analogy with (3.5), by the introduction of a magnetic voltage state $\mathbf{U}_{\mathrm{m}} = \frac{1}{s\mu}\mathbf{C}_{\mathrm{i}}\mathbf{M}$,

$$\begin{pmatrix} s\mu\mathbf{L} & \mathbf{1} & \mathbf{K} & \mathbf{0} \\ -\mathbf{1} & s\epsilon\mathbf{C} & \mathbf{0} & \mathbf{0} \\ -\mathbf{K} & \mathbf{0} & s\epsilon\mathbf{L} & \mathbf{1} \\ \mathbf{0} & \mathbf{0} & -\mathbf{1} & s\mu\mathbf{C} \end{pmatrix} \begin{pmatrix} \mathbf{I} \\ \mathbf{U} \\ \mathbf{M} \\ \mathbf{U}_{\mathrm{m}} \end{pmatrix}. \tag{5.6}$$

This system can determine the stored energy of each region with the same approximation used in (3.7). For simplicity, we consider non-dispersive material models with a single Lorentz resonance in the permittivity. Multiple Lorentz resonances and temporal dispersion in the permeability are analyzed similarly and are not detailed here. It is sufficient to use differentiation with respect to the Laplace parameter s for the non-dispersive cases to illustrate the method, giving

$$\begin{pmatrix} \mu\mathbf{L} + \omega\mu\mathbf{L}' & \mathbf{0} & -j\mathbf{K}' & \mathbf{0} \\ \mathbf{0} & \epsilon\mathbf{C} + \omega\epsilon\mathbf{C}' & \mathbf{0} & \mathbf{0} \\ j\mathbf{K}' & \mathbf{0} & \epsilon\mathbf{L} + \omega\epsilon\mathbf{L}' & \mathbf{0} \\ \mathbf{0} & \mathbf{0} & \mathbf{0} & \mu\mathbf{C} + \omega\mu\mathbf{C}' \end{pmatrix} \tag{5.7}$$

with $\mathbf{L}'$ as in (3.8), $\mathbf{C}' = -\mathbf{C}\mathbf{C}'_i\mathbf{C}$ as in (3.9), and

$$K'_{p,mn} = \kappa'\kappa \int_{\partial\Omega_p} \int_{\partial\Omega_p} \boldsymbol{\psi}_n(\boldsymbol{r}_1) \cdot \boldsymbol{\psi}_m(\boldsymbol{r}_2) \times (\boldsymbol{r}_1 - \boldsymbol{r}_2)G \,\mathrm{dS}_1\,\mathrm{dS}_2, \tag{5.8}$$

where we used

$$\frac{\partial}{\partial\kappa}\nabla_2 G = \nabla_2\frac{\partial}{\partial\kappa}G = -\nabla_2\frac{\mathrm{e}^{-\kappa R}}{4\pi} = -\frac{\kappa\mathrm{e}^{-\kappa R}(\boldsymbol{r}_1 - \boldsymbol{r}_2)}{4\pi R} = -\kappa(\boldsymbol{r}_1 - \boldsymbol{r}_2)G. \tag{5.9}$$

The $\mathbf{K}'$ term in vacuum is recognized as being proportional to the $\mathbf{K}_2$ term used in [37], see also [38]. The terms that contribute to the stored energy are expanded in the wavenumber k in [36] and it is shown that the $\mathbf{K}_1$-term and the potentially coordinate dependent terms $\mathbf{K}_3$ and $\mathbf{K}_4$ used in [37] are one order smaller than the $\mathbf{K}_2$-term. These terms are not present in the state-space based approach presented here. The contribution to the stored energy from the region Ω_p is finally given by the real part of the quadratic form

$$\begin{pmatrix} \mathbf{I} \\ \mathbf{U} \\ \mathbf{M} \\ \mathbf{U}_\mathrm{m} \end{pmatrix}^\mathrm{H} \begin{pmatrix} \mu\mathbf{L} + \omega\mu\mathbf{L}' & \mathbf{0} & -j\mathbf{K}' & \mathbf{0} \\ \mathbf{0} & \epsilon\mathbf{C} + \omega\epsilon\mathbf{C}' & \mathbf{0} & \mathbf{0} \\ j\mathbf{K}' & \mathbf{0} & \epsilon\mathbf{L} + \omega\epsilon\mathbf{L}' & \mathbf{0} \\ \mathbf{0} & \mathbf{0} & \mathbf{0} & \mu\mathbf{C} + \omega\mu\mathbf{C}' \end{pmatrix} \begin{pmatrix} \mathbf{I} \\ \mathbf{U} \\ \mathbf{M} \\ \mathbf{U}_\mathrm{m} \end{pmatrix}$$

$$= \mathbf{I}^\mathrm{H}\left(\mu\mathbf{L} + \omega\mu\mathbf{L}' + \frac{\epsilon}{|\omega\epsilon|^2}\mathbf{C} - \frac{\omega\epsilon}{|\omega\epsilon|^2}\mathbf{C}'\right)\mathbf{I} + \mathbf{M}^\mathrm{H}\left(\epsilon\mathbf{L} + \omega\epsilon\mathbf{L}' + \frac{\mu}{|\omega\mu|^2}\mathbf{C} - \frac{\omega\mu}{|\omega\mu|^2}\mathbf{C}'\right)\mathbf{M}$$

$$- j\mathbf{I}^\mathrm{H}\mathbf{K}'\mathbf{M} + j\mathbf{M}^\mathrm{H}\mathbf{K}'\mathbf{I} = \begin{pmatrix} \mathbf{I} \\ \mathbf{M} \end{pmatrix}^\mathrm{H} \begin{pmatrix} \mathbf{X}' & -j\mathbf{K}' \\ j\mathbf{K}' & \mathbf{X}' \end{pmatrix} \begin{pmatrix} \mathbf{I} \\ \mathbf{M} \end{pmatrix} \tag{5.10}$$

and the total stored energy by summation over all regions.

The expression (5.10) resembles the stored energy from electric and magnetic current densities [36, 37, 38]. The stored energies in [36, 37, 38] are derived from the subtraction of the far-field in a non-dispersive homogeneous background as in (2.2). The equivalence principle states that the fields generated by currents at $\partial\Omega_n$ vanish outside Ω_n and for that reason produces the total energy in Ω_n. The exterior region is an exception for which the energy produced is similar to the case of far-field subtraction. Consequently, the stored energy (5.10) resembles (2.2) with spatially dependent permittivity and permeability in the energy density terms, and the exterior permittivity in the subtracted far-field energy term, for small structures. The expressions differ for larger structures, where $\mathbf{K}_1$ together with the coordinate dependent terms in [36] contribute.

Figs. 7 and 8 depicts Q-factors $Q_{\widetilde{\mathbf{X}}'}$ based on the energy expressions (5.10) for multilayer structures. Fig. 7 shows Q-factors for a cylindrical dipole embedded in a dielectric cylinder. The figure contains two cases, when the permittivity of the cylinder is higher than the background, and when the permittivity of the background is higher than the cylinder. For both cases $Q_{\widetilde{\mathbf{X}}'}$ agrees very well with $Q_{Z_\mathrm{in}^\mathrm{B}}$ and $Q_{Z'_\mathrm{in}}$. However, $Q_{Z_\mathrm{in}^\mathrm{B}}$ and $Q_{Z'_\mathrm{in}}$ have slightly lower values than $Q_{\widetilde{\mathbf{X}}'}$ for $\{\epsilon_1, \epsilon_2\} = \{10, 1\}$ at higher frequencies. Fig. 8 instead shows what occurs when the dielectric cylinder encasing the dipole varies in size for the two cases. The Q-factors agree well except for higher frequencies when the cylinder is large. There is also a dip in $Q_{Z'_\mathrm{in}}$ at $0.2\ell/\lambda$ for cylinder size $2.6\ell \times 1.6\ell$.
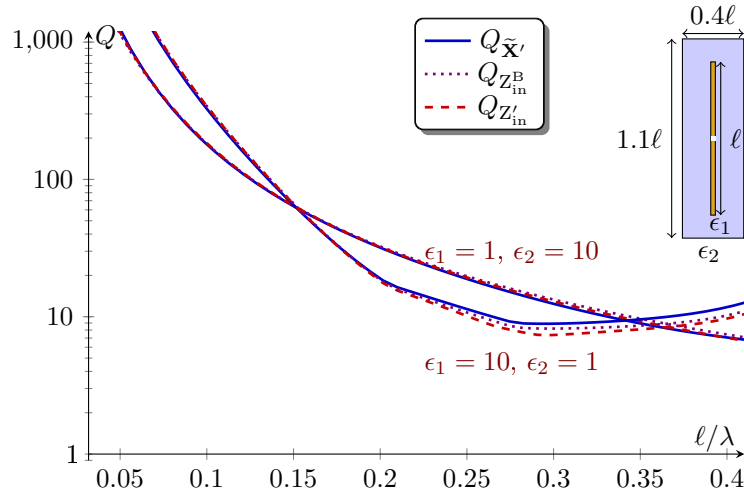
Figure 7: Q-factors for a cylindrical dipole with length ℓ, width $\ell/100$, fed at the center, and placed in a dielectric cylinder with permittivity ϵ_1 and background permittivity ϵ_2. The cylinder has height 1.1ℓ and diameter 0.4ℓ. The Q-factors are computed using (5.10), Brune synthesized circuits [21], and (A.1) for the two cases $\{\epsilon_1, \epsilon_2\} = \{1, 10\}$ and $\{\epsilon_1, \epsilon_2\} = \{10, 1\}$.

The piecewise inhomogeneous case can be expanded to temporally dispersive permittivity as was done for homogeneous media in Sec. 4.1. The system matrix (5.6) is expanded to a first order state-space model for the Lorentz model (4.1) in analog with (4.4). However, the magnetic currents give rise to the states $\mathbf{U}_\mathrm{m}, \mathbf{P}_\mathrm{m}, \dot{\mathbf{P}}_\mathrm{m}$ in addition to the voltage $\mathbf{U}$ and polarization states $\mathbf{P}$ and $\dot{\mathbf{P}}$ used in (4.4). The resulting system matrix is

$$
\widetilde{\mathbf{Z}}\tilde{\mathbf{I}} = \begin{pmatrix}
s\mu\mathbf{L} & 1 & \mathbf{K} & 0 & 0 & 0 & 0 & 0 \\
-1 & s\epsilon_\infty\mathbf{C} & 0 & 0 & 0 & 1\alpha & 0 & 0 \\
-\mathbf{K} & 0 & s\epsilon_\infty\mathbf{L} & 1 & 0 & 0 & 0 & 1\alpha \\
0 & 0 & -1 & s\mu\mathbf{C} & 0 & 0 & 0 & 0 \\
0 & 0 & 0 & 0 & s\mathbf{C}_\mathrm{i} & -\beta\mathbf{C}_\mathrm{i} & 0 & 0 \\
0 & -1\alpha & 0 & 0 & \beta\mathbf{C}_\mathrm{i} & (s\delta+\gamma)\mathbf{C}_\mathrm{i} & 0 & 0 \\
0 & 0 & 0 & 0 & 0 & 0 & s\mathbf{L}_\mathrm{i} & -\beta\mathbf{L}_\mathrm{i} \\
0 & 0 & -1\alpha & 0 & 0 & 0 & \beta\mathbf{L}_\mathrm{i} & (s\delta+\gamma)\mathbf{L}_\mathrm{i}
\end{pmatrix}
\begin{pmatrix}
\mathbf{I} \\ \mathbf{U} \\ \mathbf{M} \\ \mathbf{U}_\mathrm{m} \\ \mathbf{P} \\ \dot{\mathbf{P}} \\ \mathbf{P}_\mathrm{m} \\ \dot{\mathbf{P}}_\mathrm{m}
\end{pmatrix}, \quad (5.11)
$$

where we used

$$
(s\epsilon\mathbf{L} + \frac{\mathbf{C}_\mathrm{i}}{s\mu})\mathbf{M} = (s\epsilon_\infty\mathbf{L} + \frac{\mathbf{C}_\mathrm{i}}{s\mu} + \frac{s\alpha^2}{\chi}\mathbf{L})\mathbf{M} = s\epsilon_\infty\mathbf{L}\mathbf{M} + \mathbf{U}_\mathrm{m} + \alpha\dot{\mathbf{P}}_\mathrm{m}, \quad (5.12)
$$

and $s\alpha\mathbf{L}\mathbf{M} = \chi\dot{\mathbf{P}}_\mathrm{m} = \chi s\mathbf{P}_\mathrm{m}\beta^{-1}$ with $\mathbf{L}\mathbf{M}\alpha = \chi\mathbf{P}_\mathrm{m}\beta^{-1}$ to get

$$
\alpha\mathbf{L}\mathbf{M} = (\beta^2 + s\gamma + s^2\delta)\mathbf{P}_\mathrm{m}\beta^{-1} = \beta\mathbf{P}_\mathrm{m} + (\gamma + s\delta)\dot{\mathbf{P}}_\mathrm{m}. \quad (5.13)
$$

From here the electric and magnetic terms are analyzed as in 4.2.

Fig. 9 displays Q-factors calculated for a cylindrical dipole encased in both a dielectric cylinder with dispersive permittivity in a normal background and a vacuum cylinder in a dispersive background. The dispersive permittivity is modeled by the Lorentz model (4.1). For the case when the background is dispersive and the cylinder is vacuum, the Q-factors agree well. For the second case, when the cylinder is dispersive, $Q_{\widetilde{\mathbf{X}}'}$ and $Q_{Z_\mathrm{in}^\mathrm{B}}$ agree for the whole interval. However, $Q_{Z_\mathrm{in}'}$ has a dip around 0.2 to 0.35ℓ. This is most likely caused by multiple resonances in the input impedance.

Figure 8: Q-factors for a cylindrical dipole with length ℓ, width $\ell/100$, fed at the center, and placed in a dielectric cylinder with permittivity ϵ_1 and background permittivity ϵ_2. The cylinder has heights $\{1.4, 2.6, 3.8, 5\}\ell$ and diameters $\{0.4, 1.6, 2.8, 4\}\ell$ (◖). The Q-factors are computed using (5.10), Brune synthesized circuits [21], and (A.1) for the two cases $\{\epsilon_1, \epsilon_2\} = \{1, 2\}$ and $\{\epsilon_1, \epsilon_2\} = \{2, 1\}$.

5.2 Inhomogeneous media

To handle fully inhomogeneous background media we use volume integral equations [10], the implementation of which is much more arduous than surface based integral equations. However, the method for constructing the state-space system and calculating the stored energy is principally the same. For completeness, we present here the analysis needed to calculate the stored energy with volume integral equations.

Consider a dielectric body with relative permittivity $\epsilon_{\mathrm{r}}(\boldsymbol{r})$. The volume EFIE is

$$\boldsymbol{E}(\boldsymbol{r}_1) = \boldsymbol{E}_{\mathrm{i}}(\boldsymbol{r}_1) - k^2 \int_\Omega \mathbf{G}(\boldsymbol{r}_1 - \boldsymbol{r}_2) \cdot (1 - \epsilon_{\mathrm{r}}(\boldsymbol{r}_2))\boldsymbol{E}(\boldsymbol{r}_2)\,\mathrm{dV}_2, \tag{5.14}$$

where $\mathbf{G} = (\mathbf{1} + k^{-2}\nabla\nabla)G$ is the Green dyadic, k the free-space wavenumber, and $\boldsymbol{E}_{\mathrm{i}}$ the incident electric field. Introduce the contrast current density $\boldsymbol{J} = \kappa(1 - \epsilon_{\mathrm{r}})\boldsymbol{E}$ to reformulate (5.14) to an integral equation in that quantity

$$\frac{\boldsymbol{J}(\boldsymbol{r}_1)}{\kappa(1 - \epsilon_{\mathrm{r}}(\boldsymbol{r}_1))} = \boldsymbol{E}_{\mathrm{i}}(\boldsymbol{r}_1) + \kappa \int_\Omega \mathbf{G}(\boldsymbol{r}_1 - \boldsymbol{r}_2) \cdot \boldsymbol{J}(\boldsymbol{r}_2)\,\mathrm{dV}_2. \tag{5.15}$$

Multiply both sides with test functions $\boldsymbol{\Psi}$ and integrate over the volume

$$\int_\Omega \frac{\boldsymbol{\Psi}(\boldsymbol{r}) \cdot \boldsymbol{J}(\boldsymbol{r})}{\kappa(1 - \epsilon_{\mathrm{r}}(\boldsymbol{r}))}\,\mathrm{dV} = \int_\Omega \boldsymbol{\Psi}(\boldsymbol{r}) \cdot \boldsymbol{E}_{\mathrm{i}}(\boldsymbol{r})\,\mathrm{dV}$$
$$+ \int_\Omega \int_\Omega \kappa G(\boldsymbol{r}_1 - \boldsymbol{r}_2)\boldsymbol{\Psi}(\boldsymbol{r}_1) \cdot \boldsymbol{J}(\boldsymbol{r}_2) + \frac{1}{\kappa}G(\boldsymbol{r}_1 - \boldsymbol{r}_2)\nabla_1 \cdot \boldsymbol{\Psi}(\boldsymbol{r}_1)\nabla_2 \cdot \boldsymbol{J}(\boldsymbol{r}_2)\,\mathrm{dV}_1\,\mathrm{dV}_2, \tag{5.16}$$

where we split the Green's dyadic $\mathbf{G}$ into two parts. The differentiated term is partially integrated to reduce the singularity of the Green's function

$$\int_\Omega \int_\Omega \boldsymbol{J}(\boldsymbol{r}_1) \cdot \nabla\nabla G \cdot \boldsymbol{J}(\boldsymbol{r}_2)\,\mathrm{dV}_1\,\mathrm{dV}_2 = - \int_\Omega \int_\Omega \nabla_1 \cdot \boldsymbol{J}(\boldsymbol{r}_1)G\nabla_2 \cdot \boldsymbol{J}(\boldsymbol{r}_2)\,\mathrm{dV}_1\,\mathrm{dV}_2. \tag{5.17}$$
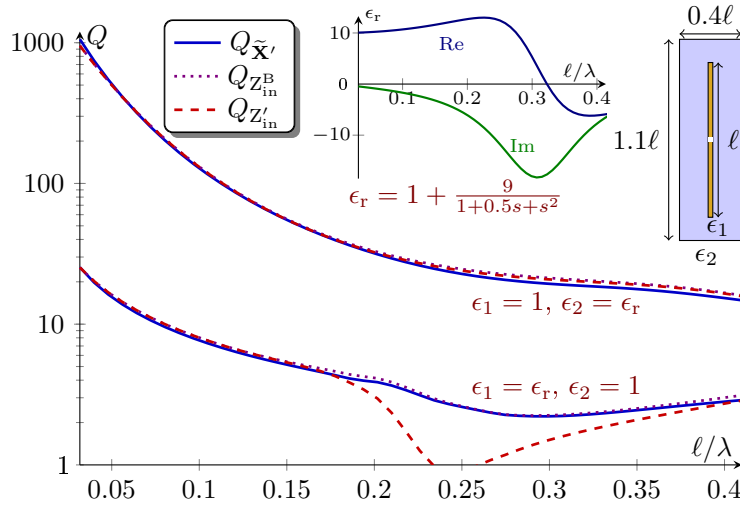
Figure 9: Q-factors for a cylindrical dipole with length ℓ, width $\ell/100$, fed at the center, and placed in a dielectric cylinder with permittivity ϵ_1 and background permittivity ϵ_2. The cylinder has height 1.1ℓ and diameter 0.4ℓ. The Q-factors are computed using (5.10), Brune synthesized circuits [21], and (A.1) for the two cases $\{\epsilon_1, \epsilon_2\} = \{1, \epsilon_r\}$ and $\{\epsilon_1, \epsilon_2\} = \{\epsilon_r, 1\}$, $\epsilon_r = 1 + 9/(1 + 0.5s + s^2)$.

To obtain the MoM formulation we expand the contrast current density $\boldsymbol{J}$ in basis functions $\boldsymbol{\Psi}_n$ as

$$I_n = \int_\Omega \boldsymbol{\Psi}_n(\boldsymbol{r}) \cdot \boldsymbol{J}(\boldsymbol{r}) \, \mathrm{dV} = \int \boldsymbol{\Psi}_n(\boldsymbol{r}) \cdot \kappa\big(1 - \epsilon_r(\boldsymbol{r})\big)\boldsymbol{E}(\boldsymbol{r}) \, \mathrm{dV}. \tag{5.18}$$

This enables the introduction of matrix quantities similar to those used in (3.1), and thus, the construction of the state-space system. The inductance matrix is defined as

$$L_{mn} = \int_\Omega \int_\Omega G(\boldsymbol{r}_1 - \boldsymbol{r}_2)\boldsymbol{\Psi}_m(\boldsymbol{r}_1) \cdot \boldsymbol{\Psi}_n(\boldsymbol{r}_2) \, \mathrm{dV}_1 \, \mathrm{dV}_2, \tag{5.19}$$

the capacitance matrix as

$$C_{imn} = \int_\Omega \int_\Omega G(\boldsymbol{r}_1 - \boldsymbol{r}_2)\nabla_1 \cdot \boldsymbol{\Psi}_m(\boldsymbol{r}_1)\nabla_2 \cdot \boldsymbol{\Psi}_n(\boldsymbol{r}_2) \, \mathrm{dV}_1 \, \mathrm{dV}_2, \tag{5.20}$$

and the material matrix as

$$M_{mn} = \int_\Omega \frac{\boldsymbol{\Psi}_m(\boldsymbol{r}) \cdot \boldsymbol{\Psi}_n(\boldsymbol{r})}{1 - \epsilon_r(\boldsymbol{r})} \, \mathrm{dV}. \tag{5.21}$$

With these three matrices equation (5.16) can be written as the second order system

$$\Big(s\mu_0\mathbf{L} + \frac{\mathbf{C}_i + \mathbf{M}}{s\epsilon_0}\Big)\mathbf{I} = \mathbf{V}. \tag{5.22}$$

Similarly to previous sections it can be transformed to the first order state-space model by the introduction of a voltage state $\mathbf{U} = \frac{1}{s\epsilon_0}(\mathbf{C}_i + \mathbf{M})\mathbf{I}$

$$\begin{pmatrix} s\mu_0\mathbf{L} & \mathbf{1} \\ -\mathbf{1} & s\epsilon_0(\mathbf{C}_i + \mathbf{M})^{-1} \end{pmatrix}\begin{pmatrix} \mathbf{I} \\ \mathbf{U} \end{pmatrix} = \begin{pmatrix} \mathbf{V} \\ \mathbf{0} \end{pmatrix}. \tag{5.23}$$

Finally, the stored energy is given by the quadratic form of the frequency differentiation of the state-space matrix

$$W = \frac{\mathrm{Re}}{4}\begin{pmatrix} \mathbf{I} \\ \mathbf{U} \end{pmatrix}^{\mathrm{H}}\begin{pmatrix} \mu_0(\mathbf{L} + \omega\mathbf{L}') & \mathbf{0} \\ \mathbf{0} & \epsilon_0(\mathbf{C}_i + \mathbf{M})^{-1} - \epsilon_0\omega(\mathbf{C}_i + \mathbf{M})^{-1}\mathbf{C}_i'(\mathbf{C}_i + \mathbf{M})^{-1} \end{pmatrix}\begin{pmatrix} \mathbf{I} \\ \mathbf{U} \end{pmatrix}$$

$$= \frac{\mathrm{Re}}{4}\mathbf{I}^{\mathrm{H}}\big(\mu_0(\mathbf{L} + \omega\mathbf{L}') + \frac{1}{\omega^2\epsilon_0}(\mathbf{C}_i + \mathbf{M} - \omega\mathbf{C}_i')\big)\mathbf{I} = \frac{1}{4}\mathbf{I}^{\mathrm{H}}\frac{\partial\mathbf{X}}{\partial\omega}\mathbf{I}. \tag{5.24}$$

6   Conclusions

State-space models for the input impedance based on the integral equations EFIE and MFIE have been used to determine the stored electromagnetic energy for small antennas. These expressions have been calculated by synthesizing first order state-space models. The stored energy is expressed as a quadratic form of the frequency differentiated system matrix and the states. This quadratic form is advantageous because it enables us to utilize these stored energy expressions in fast and efficient optimization techniques [7, 12, 23, 24].

For the free-space case it is shown in Sec. 3 that the proposed expression is identical to the stored energy introduced by Vandenbosch [49], see also [31]. This energy expression has been verified for several antennas with good results [12, 13, 21, 32]. In [25], it is, however, shown that the quadratic form can be indefinite for sufficiently large structures. This partly questions the validity of the energy expression, although the same problem appears in the commonly used stored energy [59] defined by subtraction of the far-field [22]. The energy expressions presented here are restricted to electrically small antennas where they are positive definite. The open question of defining and efficiently evaluating the stored energy for electrically large structures remains, as of yet, unsolved.

In Sec. 4 the state-space models are generalized to temporally dispersive background media. The results produced by the state-space method seem to be reliable and produce similar values as Brune circuit synthesis [21] and differentiation of the input impedance $Q_{Z'_{in}}$ for single resonance cases. However, the main advantage over other contemporary methods is that the state-space model is written as a quadratic form in the current, and hence enables fast and effective use in antenna current optimization [8, 12, 20, 23, 24, 34].

The state-space model was further generalized to piecewise inhomogeneous media in Sec. 5. Here it was shown that the method is stable for cases where there are lossy media present but radiation still exists. These cases are of special interest since they have similarities with applications such as implanted antenna system. By offering a stable method of calculating the Q-factor for inhomogeneous media the state-space method opens up avenues of research for calculating optimal Q values for application based cases. This suggests the possibility to construct Q-factor bounds for more applications than free space [23, 24] and infinite ground planes [47].

Acknowledgment

Appendix A   Q-factors $Q_{Z'_{in}}$ and Q_{Γ_0}

By taking the frequency derivative of the input impedance, the stored energy can be approximated through the Q-factor [43, 59],

$$Q_{Z'_{in}} = \frac{\omega}{2R_{in}(\omega)}|Z'_{in0}(\omega)|, \tag{A.1}$$

where Z_{in0} is the input impedance tuned to resonance. This simple expression (A.1) gives an accurate measure of the fractional bandwidth, but can overestimate the bandwidth for multiple resonance cases [26, 46].

The corresponding fractional bandwidth, B, is

$$B \approx \frac{2}{Q}\frac{\Gamma_0}{\sqrt{1-\Gamma_0^2}}, \tag{A.2}$$

for single resonance antennas [59], where Γ_0 denotes the threshold for the reflection coefficient. The relationship between the fractional bandwidth and Q-factor (A.2) for the RLC resonance circuit

can also be used to define an equivalent Q-factor for a given threshold level Γ_0 *i.e.*,

$$Q_{\Gamma_0} = \frac{2}{B_{\Gamma_0}} \frac{\Gamma_0}{\sqrt{1 - \Gamma_0^2}}, \tag{A.3}$$

where B_{Γ_0} denotes the fractional bandwidth for the threshold Γ_0.

Appendix B MoM impedance matrix

The MoM impedance matrix is divided into two parts in (3.1). This decomposition is non-unique and $\mathbf{Z}$ can alternatively be divided as

$$\mathbf{Z} = j\omega\mu_0\mathbf{L} + \frac{1}{j\omega\epsilon_0}\mathbf{C}_i + \eta_0\mathbf{R} \tag{B.1}$$

for the free space case, where

$$L_{mn} = \int_{\partial\Omega}\int_{\partial\Omega} \boldsymbol{\psi}_{m1} \cdot \boldsymbol{\psi}_{n2} \frac{\cos(kR_{12})}{4\pi R_{12}} \, \mathrm{dS}_1 \, \mathrm{dS}_2, \tag{B.2}$$

$$C_{imn} = \int_{\partial\Omega}\int_{\partial\Omega} \nabla_1 \cdot \boldsymbol{\psi}_{m1} \nabla_2 \cdot \boldsymbol{\psi}_{n2} \frac{\cos(kR_{12})}{4\pi R_{12}} \, \mathrm{dS}_1 \, \mathrm{dS}_2, \tag{B.3}$$

and

$$R_{mn} = \int_{\partial\Omega}\int_{\partial\Omega} (k\boldsymbol{\psi}_{m1} \cdot \boldsymbol{\psi}_{n2} - \frac{1}{k}\nabla_1 \cdot \boldsymbol{\psi}_{m1} \nabla_2 \cdot \boldsymbol{\psi}_{n2}) \frac{\sin(kR_{12})}{4\pi R_{12}} \, \mathrm{dS}_1 \, \mathrm{dS}_2, \tag{B.4}$$

Here, $\boldsymbol{\psi}_{ni}$ is a short hand notation for basis functions $\boldsymbol{\psi}_n(\boldsymbol{r}_i)$ with $n = 1, ..., N$, $i = 1, 2$, $\boldsymbol{r}_i$ denotes the position vector, and $R_{12} = |\boldsymbol{r}_1 - \boldsymbol{r}_2|$.

Appendix References

[1]   A. Alù et al. "Epsilon-near-zero metamaterials and electromagnetic sources: tailoring the radiation phase pattern". *Physical Review B* 75.15 (2007), p. 155410.

[2]   S. Arslanagic, R. W. Ziolkowski, and O. Breinbjerg. "Analytical and numerical investigation of the radiation and scattering from concentric metamaterial cylinders excited by an electric line source". *Radio Sci.* 42.6 (2007).

[3]   S. R. Best. "Electrically small resonant planar antennas: optimizing the quality factor and bandwidth." *IEEE Antennas Propag. Mag.* 57.3 (2015), pp. 38–47.

[4]   J. G. van Bladel. *Electromagnetic Fields*. Second Edition. IEEE Press, 2007.

[5]   O. Brune. "Synthesis of a finite two-terminal network whose driving-point impedance is a prescribed function of frequency". *MIT J. Math. Phys.* 10 (1931), pp. 191–236.

[6]   C. Caloz. "Metamaterial dispersion engineering concepts and applications". *Proceedings of the IEEE* 99.10 (2011), pp. 1711–1719.

[7]   M. Capek, M. Gustafsson, and K. Schab. "Minimization of antenna quality factor". *arXiv preprint arXiv:1612.07676* (2016).

[8]   M. Capek, L. Jelinek, and G. A. E. Vandenbosch. "Stored electromagnetic energy and quality factor of radiating structures". *Proc. R. Soc. A* 472.2188 (2016).

[9]   F. Capolino, ed. *Theory and Phenomena of Metamaterials*. CRC Press, 2009.

[10] W. C. Chew, M. S. Tong, and B. Hu. *Integral equation methods for electromagnetic and elastic waves*. Vol. 12. Morgan & Claypool, 2008.

[11] L. J. Chu. "Physical limitations of omnidirectional antennas". *J. Appl. Phys.* 19 (1948), pp. 1163–1175.

[12] M. Cismasu and M. Gustafsson. "Antenna bandwidth optimization with single frequency simulation". *IEEE Trans. Antennas Propag.* 62.3 (2014), pp. 1304–1311.

[13] M. Cismasu and M. Gustafsson. "Multiband antenna Q optimization using stored energy expressions". *IEEE Antennas and Wireless Propagation Letters* 13.2014 (2014), pp. 646–649.

[14] R. E. Collin and S. Rothschild. "Evaluation of antenna Q". *IEEE Trans. Antennas Propag.* 12 (1964), pp. 23–27.

[15] N. Engheta and R. W. Ziolkowski. *Metamaterials: physics and engineering explorations.* John Wiley & Sons, 2006.

[16] R. L. Fante. "Quality factor of general antennas". *IEEE Trans. Antennas Propag.* 17.2 (1969), pp. 151–155.

[17] W. Geyi. "A method for the evaluation of small antenna Q". *IEEE Trans. Antennas Propag.* 51.8 (2003), pp. 2124–2129.

[18] W. Geyi. "Physical limitations of antenna". *IEEE Trans. Antennas Propag.* 51.8 (2003), pp. 2116–2123.

[19] W. Geyi. *Foundations of Applied Electrodynamics.* John Wiley & Sons, 2011.

[20] M. Gustafsson, J. Friden, and D. Colombi. "Antenna current optimization for lossy media with near field constraints". *Antennas and Wireless Propagation Letters, IEEE* 14 (2015), pp. 1538–1541.

[21] M. Gustafsson and B. L. G. Jonsson. "Antenna Q and stored energy expressed in the fields, currents, and input impedance". *IEEE Trans. Antennas Propag.* 63.1 (2015), pp. 240–249.

[22] M. Gustafsson and B. L. G. Jonsson. "Stored electromagnetic energy and antenna Q". *Progress In Electromagnetics Research (PIER)* 150 (2015), pp. 13–27.

[23] M. Gustafsson and S. Nordebo. "Optimal antenna currents for Q, superdirectivity, and radiation patterns using convex optimization". *IEEE Trans. Antennas Propag.* 61.3 (2013), pp. 1109–1118.

[24] M. Gustafsson et al. "Antenna current optimization using MATLAB and CVX". *FERMAT* 15.5 (2016), pp. 1–29.

[25] M. Gustafsson, M. Cismasu, and B. L. G. Jonsson. "Physical bounds and optimal currents on antennas". *IEEE Trans. Antennas Propag.* 60.6 (2012), pp. 2672–2681.

[26] M. Gustafsson and S. Nordebo. "Bandwidth, Q factor, and resonance models of antennas". *Prog. Electromagn. Res.* 62 (2006), pp. 1–20.

[27] M. Gustafsson, D. Tayli, and M. Cismasu. "Physical bounds of antennas". In: *Handbook of Antenna Technologies.* Ed. by Z. N. Chen. Springer-Verlag, 2015, pp. 1–32.

[28] M. Gustafsson, D. Tayli, and M. Cismasu. *Q factors for antennas in dispersive media.* Tech. rep. LUTEDX/(TEAT-7232)/1–24/(2014). Lund University, 2014.

[29] T. V. Hansen, O. S. Kim, and O. Breinbjerg. "Properties of sub-wavelength spherical antennas with arbitrarily lossy magnetodielectric cores approaching the Chu lower bound". *IEEE Trans. Antennas Propag.* 62.3 (2014), pp. 1456–1460.

[30] R. F. Harrington. *Field Computation by Moment Methods.* Macmillan, 1968.

[31] R. F. Harrington and J. R. Mautz. "Control of radar scattering by reactive loading". *IEEE Trans. Antennas Propag.* 20.4 (1972), pp. 446–454.

[32] P. Hazdra, M. Capek, and J. Eichler. "Radiation Q-factors of thin-wire dipole arrangements". *Antennas and Wireless Propagation Letters, IEEE* 10 (2011), pp. 556–560.

[33] J. D. Jackson. *Classical Electrodynamics.* Third. John Wiley & Sons, 1999.

[34] L Jelinek and M Capek. "Optimal currents on arbitrarily shaped surfaces". *IEEE Trans. Antennas Propag.* 65.1 (2017), pp. 329–341.

[35] J. M. Jin. *Theory and computation of electromagnetic fields.* Wiley Online Library, 2010.

[36] B. L. G. Jonsson and M. Gustafsson. "Stored energies for electric and magnetic current densities". *arXiv preprint arXiv:1604.08572* (2016).

[37] B. L. G. Jonsson and M. Gustafsson. "Stored energies in electric and magnetic current densities for small antennas". *Proc. R. Soc. A* 471.2176 (2015), p. 20140897.

[38] O. S. Kim. "Lower bounds on Q for finite size antennas of arbitrary shape". *IEEE Trans. Antennas Propag.* 64.1 (2016), pp. 146–154.

[39] L. D. Landau and E. M. Lifshitz. *Electrodynamics of Continuous Media*. First. Pergamon Press, 1960.

[40] J. S. McLean. "A re-examination of the fundamental limits on the radiation Q of electrically small antennas". *IEEE Trans. Antennas Propag.* 44.5 (1996), pp. 672–676.

[41] F. Merli et al. "Design, realization and measurements of a miniature antenna for implantable wireless communication systems". *IEEE Trans. Antennas Propag.* 59.10 (2011), pp. 3544–3555.

[42] R. K. Moore. "Effects of a surrounding conducting medium on antenna analysis". *IEEE Trans. Antennas Propag.* 11.3 (1963), pp. 216–225.

[43] T. Ohira. "What in the world is Q?" *IEEE Microwave Magazine* 17.6 (2016), pp. 42–49.

[44] A. F. Peterson, S. L. Ray, and R. Mittra. *Computational Methods for Electromagnetics*. IEEE Press, 1998.

[45] R Ruppin. "Electromagnetic energy density in a dispersive and absorptive material". *Physics letters A* 299.2 (2002), pp. 309–312.

[46] H. Stuart, S. Best, and A. Yaghjian. "Limitations in relating quality factor to bandwidth in a double resonance small antenna". *Antennas and Wireless Propagation Letters* 6 (2007).

[47] D. Tayli and M. Gustafsson. "Physical bounds for antennas above a ground plane". *Antennas and Wireless Propagation Letters, IEEE* 15 (2016), pp. 1281–1284.

[48] S. Tretyakov. "Electromagnetic field energy density in artificial microwave materials with strong dispersion and loss". *Physics Letters A* 343.1 (2005), pp. 231–237.

[49] G. A. E. Vandenbosch. "Reactive energies, impedance, and Q factor of radiating structures". *IEEE Trans. Antennas Propag.* 58.4 (2010), pp. 1112–1127.

[50] G. A. E. Vandenbosch. "Radiators in time domain, part II: finite pulses, sinusoidal regime and Q factor". *IEEE Trans. Antennas Propag.* 61.8 (2013), pp. 4004–4012.

[51] J. Volakis, C. C. Chen, and K. Fujimoto. *Small Antennas: Miniaturization Techniques & Applications*. McGraw-Hill, 2010.

[52] J. L. Volakis and K. Sertel. *Integral Equation Methods for Electromagnetics*. SciTech Publishing Inc., 2012.

[53] O. B. Vorobyev. "Energy density of macroscopic electric and magnetic fields in dispersive medium with losses". *Progress In Electromagnetics Research B* 40 (2012), pp. 343–360.

[54] H. A. Wheeler. "Fundamental limitations of a small VLF antenna for submarines". *IRE Trans. on Antennas and Propagation* 6 (1958), pp. 123–125.

[55] J. C. Willems. "Dissipative dynamical systems part II: linear systems with quadratic supply rates". *Arch. Rational Mech. Anal.* 45.5 (1972), pp. 352–393.

[56] O. Wing. *Classical Circuit Theory*. Springer, 2008.

[57] A. D. Yaghjian. "Internal energy, Q-energy, Poynting's theorem, and the stress dyadic in dispersive material". *IEEE Trans. Antennas Propag.* 55.6 (2007), pp. 1495–1505.

[58] A. D. Yaghjian, M. Gustafsson, and B. L. G Jonsson. "Minimum Q for lossy and lossless electrically small dipole antennas". *Progress In Electromagnetics Research* 143 (2013), pp. 641–673.

[59] A. D. Yaghjian and S. R. Best. "Impedance, bandwidth, and Q of antennas". *IEEE Trans. Antennas Propag.* 53.4 (2005), pp. 1298–1324.